

Lieb and hole-doped ferrimagnetism, spiral, resonating valence-bond states, and phase separation in large- U AB_2 Hubbard chains

V. M. Martinez Alvarez¹ and M. D. Coutinho-Filho¹

¹*Departamento de Física, Laboratório de Física Teórica e Computacional,
Universidade Federal de Pernambuco, Recife 50670-901, Pernambuco, Brazil*

The ground state (GS) properties of the quasi-one-dimensional AB_2 Hubbard model are investigated taking the effects of charge and spin quantum fluctuations on equal footing. In the strong-coupling regime, we derive a low-energy Lagrangian suitable to describe the ferrimagnetic phase at half filling and the phases in the hole-doped regime. At half filling, a perturbative spin-wave analysis allows us to find the GS energy, sublattice magnetizations, and Lieb total spin per unit cell of the effective quantum Heisenberg model, in very good agreement with previous results. In the challenging hole doping regime away from half filling, we derive the corresponding t - J Hamiltonian. Under the assumption that charge and spin quantum correlations are decoupled, the evolution of the second-order spin-wave modes in the doped regime unveils the occurrence of spatially modulated spin structures and the emergence of phase separation in the presence of resonating-valence-bond states. We also calculate the doping-dependent GS energy and total spin per unit cell, in which case it is shown that the spiral ferrimagnetic order collapses at a critical hole concentration. Notably, our analytical results in the doped regime are in very good agreement with density matrix renormalization group studies, where our assumption of spin-charge decoupling is numerically supported by the formation of charge-density waves in anti-phase with the modulation of the magnetic structure.

I. INTRODUCTION

Much attention has been given to quantum phase transitions [1, 2], which are phenomena characterized by the change of the nature of the ground state (GS) driven by a non-thermal parameter: pressure, magnetic field, doping, Coulomb repulsion, or competitive interactions. In this context, the study of quasi-one-dimensional (quasi-1D) compounds with ferrimagnetic properties [3, 4] has attracted considerable theoretical and experimental interest because of their unique physical properties and very rich phase diagrams. In particular, the GS of quasi-1D quantum ferrimagnets with AB_2 or ABB' unit cell topologies (diamond or trimer chains) described by the Heisenberg or Hubbard models [5] exhibit unsaturated spontaneous magnetization, ferromagnetic and antiferromagnetic spin-wave modes, effect of quantum fluctuations, and field-dependent magnetization plateaus, among several other features of interest.

Of special interest is the topological origin of GS magnetic long-range order associated with the unit cell structure of the lattice [5–12]. These studies have been motivated and supported by exact solutions and rigorous results [13–18]; in particular, at half filling, the total spin per unit cell obeys Lieb-Mattis [13] (Heisenberg model) or Lieb's theorem [15] (Hubbard model). On the other hand, it has been verified that the ferrimagnetic GS of spin-1/2 Heisenberg and Hubbard/ t - J AB_2 chains, under the effect of frustration [19–23] or doping [7, 11, 24, 25], are strongly affected by quantum fluctuations that might cause its destruction and the occurrence of new exotic phases: spiral incommensurate (IC) spin structures, Nagaoka ($U \rightarrow \infty$) and resonating-valence-bond (RVB) states, phase separation (PS), and Luttinger-liquid behavior. These features can enhance the phenomenology in comparison with a linear chain, which is dominated by the nontrivial Luttinger-liquid behavior that exhibits fractional excitations [26, 27], emergent fractionalized particles [28],

and fractional-exclusion statistic properties [29] in the spin-incoherent regime [30]. In addition, investigations of transport properties in AB_2 chains, and related structures, have also unveiled very interesting features [31].

On the experimental side, studies [32–34] of the magnetic properties of homometallic phosphate compounds of the family $A_3Cu_3(PO_4)_4$ ($A = Ca, Sr, Pb$) suggest that in these materials the line of trimers formed by spin-1/2 Cu^{+2} ions antiferromagnetically coupled do exhibit ferrimagnetism of topological origin. Further, compounds $Ca_3M_3(PO_4)_4$ ($M = Ni, Co$) with a wave-like layer structure built by zigzag M -chains exhibit antiferromagnetic ordering ($M = Ni$) or paramagnetic behavior ($M = Co$) [35]. On the other hand, bimetallic compounds, such as $CuMn(S_2C_2O_2)_2 \cdot 7.5H_2O$ [36], can be modeled [36–38] by alternate spin-1/2 - spin-5/2 chains and support interesting field-induced quantum critical points and Luttinger-liquid phase [37]. In addition, frustrated diamond (AB_2 topology) chains can properly model the compound azurite, $Cu_3(CO_3)_2(OH)_2$, in which case the occurrence of the 1/3 magnetization plateau is verified at high fields [39] in agreement with topological arguments [40] akin to those invoked in the quantum Hall effect. The spin-1/2 trimer chain compound $Cu_3(P_2O_6OH)_2$, with antiferromagnetic interactions only, also display the 1/3 magnetization plateau [41]. Interestingly, it has been established that in azurite the magnetization plateau is a dimer-monomer state [42], i.e., the chain is formed by pairs of $S = 1/2$ monomers and $S = 0$ dimers, with a small local polarization of the diamond spins [43], in agreement with density functional theory [44]. These dimer-monomer states have been found previously in the context of modeling frustrated AB_2 chains [45–47], and confirmed through a modeling using quantum rotors [48]. In contrast to azurite, whose dimers appear perpendicular to the chain direction, in the spin-1/2 inequilateral diamond-chain compounds [49] $A_3Cu_3AlO_2(SO_4)_4$ ($A = K, Rb, Cs$), the magnetic exchange interactions force the dimers to lie along the sides of the diamond cells and the monomers form a 1D

Heisenberg chain. In fact, the low-energy excitations of these new compounds have been probed and a Tomonaga-Luttinger spin liquid behavior identified [50]. It is worth mentioning that strongly frustrated AB_2 chains can exhibit ladder-chain decoupling [20], in which case the ladder is formed via the coupling between dimer spins in neighboring AB_2 unit cells.

On the other hand, besides the above-mentioned quasi-1D compounds and related magnetic properties, considerable efforts have been devoted to the study of superconductivity and intriguing magnetic/charge ordered phases in doped materials [51, 52], in particular the formation of spin-gapped states in compounds such as the family of doped $(\text{La, Sr, Ca})_{14}\text{Cu}_{24}\text{O}_{41}$. This compound is formed by one-dimensional CuO_2 diamond chains, (Sr, Ca) layers, and two-leg Cu_2O_3 ladders [53]. These results certainly stimulate experimental and theoretical investigations of quasi-1D compounds in the hole-doped regime, which is the main focus of our work, as described in the following.

In this work, we shall employ an analytical approach suitable to describe the strongly coupled Hubbard model on doped AB_2 chains, which were the object of recent numerical studies through density matrix renormalization group (DMRG) techniques [25]. Our functional integral approach, combined with a perturbative expansion in the strong-coupling regime, was originally proposed to study the doped Hubbard chain [54], and later adapted to describe various doped-induced phase transitions in the $U = \infty$ AB_2 Hubbard chain [55]. In addition, this approach was used to describe the doped strongly coupled Hubbard model on the honeycomb lattice [56], whose results are very rewarding, particularly those for the GS energy and magnetization in the doped regime, which compare very well with Grassmann tensor product numerical studies [57].

The paper is organized as follows: in Sec. II we review the functional integral representation of the Hubbard Hamiltonian in terms of Grassmann fields (charge degrees of freedom) and spin $SU(2)$ gauge fields (spin degrees of freedom). In Sec. III we diagonalize the Hamiltonian associated with the charge degree of freedom and obtain a perturbative low-energy theory suitable to describe the ferrimagnetic phase at half filling and the phases in the hole-doped regimes. In Sec. IV, we show that the resultant Hamiltonian at half filling and large- U maps onto the spin-1/2 quantum Heisenberg model. In this regime, a perturbative series expansions in powers of $1/S$ of the spin-wave modes is presented, which allows us to calculate the GS energy, sublattice magnetizations, and Lieb GS total spin per unit cell in very good agreement with previous estimates. In Sec. V, we derive the low-energy effective t - J Hamiltonian, which accounts for both charge and spin quantum fluctuations. We also present the evolution of the second-order spin-wave modes, GS energy and total spin per unit cell under hole doping, thus identifying the occurrence of spatially modulated spin structures, with non-zero and zero GS total spin, and phase separation involving the later spin structure and RVB states at hole concentration $1/3$. Remarkably, these predictions are in very good agreement with the DMRG data reported in Ref. [25]. Lastly, in Sec. VI, we present a summary and concluding remarks concerning the reported results.

II. FUNCTIONAL-INTEGRAL REPRESENTATION

The Hamiltonian of the one-band Hubbard model on chains with AB_2 unit cell topology is given by [7, 8, 10]:

$$\mathcal{H} = - \sum_{\langle i\alpha, j\beta \rangle \sigma} \{t_{ij}^{\alpha\beta} \hat{c}_{i\alpha\sigma}^\dagger \hat{c}_{j\beta\sigma} + \text{H.c.}\} + U \sum_{i\alpha} \hat{n}_{i\alpha\uparrow} \hat{n}_{i\alpha\downarrow}, \quad (1)$$

where $i = 1, \dots, N_c$ ($= N/3$) is the specific position of the unit cell, whose length is set to unity, N_c (N) is the number of cells (sites), $\alpha, \beta = A, B_1, B_2$ denote the type of site within the unit cell, $\hat{c}_{i\alpha\sigma}^\dagger$ ($\hat{c}_{i\alpha\sigma}$) is the creation (annihilation) operator of electrons with spin σ ($=\uparrow, \downarrow$) at site α of cell i , and $\hat{n}_{i\alpha\sigma} = \hat{c}_{i\alpha\sigma}^\dagger \hat{c}_{i\alpha\sigma}$ is the occupancy number operator. The first term in Eq. (1) describes electron hopping, with energy $t_{ij}^{\alpha\beta} \equiv t$, allowed only between nearest neighbors A - B_1 and A - B_2 linked sites of sublattices A and B (bipartite lattice), and the second one is the on-site Coulombian repulsive interaction $U > 0$, which contributes only in the case of double occupancy of the site $i\alpha$.

At this point, it is instructive to digress on some fundamental aspects of the formalism used in our work [54–56]. With regard to the large- U doped Hubbard chain [54], $U = \infty$ AB_2 Hubbard chain [55] and the Hubbard model on the honeycomb lattice [56], it has been shown that the particle density product in Eq. (1) can be treated through the use of a decomposition procedure, which consists in expressing $\hat{n}_{i\alpha\uparrow} \hat{n}_{i\alpha\downarrow}$ in terms of charge and spin operators:

$$\hat{n}_{i\alpha\uparrow} \hat{n}_{i\alpha\downarrow} = \frac{1}{2} \hat{\rho}_{i\alpha} - 2(\hat{\mathbf{S}}_{i\alpha} \cdot \mathbf{n}_{i\alpha})^2, \quad (2)$$

where

$$\hat{\mathbf{S}}_{i\alpha} = 1/2 \sum_{\sigma\sigma'} \hat{c}_{i\alpha\sigma'}^\dagger \boldsymbol{\sigma}_{\sigma'\sigma} \hat{c}_{i\alpha\sigma}, \quad (3)$$

and

$$\hat{\rho}_{i\alpha} = \hat{n}_{i\alpha\uparrow} + \hat{n}_{i\alpha\downarrow}, \quad (4)$$

are the spin-1/2 and charge-density operators, respectively, $\sigma_{\sigma'\sigma}$ denotes the Pauli matrix elements ($\hbar \equiv 1$), and $\mathbf{n}_{i\alpha}$ is an arbitrary unit vector. In fact, Eq. (2) follows from the identity: $\frac{1}{2} \hat{\rho}_{i\alpha} - \hat{n}_{i\alpha\uparrow} \hat{n}_{i\alpha\downarrow} = 2(\hat{S}_{i\alpha}^{x,y,z})^2 = 2(\hat{\mathbf{S}}_{i\alpha} \cdot \mathbf{n}_{i\alpha})^2$. The convenience of using the decomposition defined in Eq. (2), with explicit spin-rotational invariance for the large- U Hubbard model, was discussed at length in Refs. [54–56].

We start by using the Trotter-Suzuki formula [58, 59], which allows us to write the partition function, $\mathcal{Z} = \text{Tr}[\exp(-\beta\mathcal{H})]$, at a temperature $k_B T \equiv 1/\beta$, as $\mathcal{Z} = \text{Tr}\{\hat{T} \prod_{r=1}^M \exp[-\delta\tau \mathcal{H}(\tau_r)]\}$, where \hat{T} denotes the time-ordering operator, the total imaginary time interval is formally sliced into M discrete intervals of equal size $\delta\tau = \tau_r - \tau_{r-1}$, $r = 1, 2, \dots, M$, with $\tau_0 = 0$, and $\tau_M = \beta = M\delta\tau$, under the limits $M \rightarrow \infty$ and $\delta\tau \rightarrow 0$. We shall now introduce, between each discrete time interval, an overcomplete basis of fermionic coherent states [58, 59], $1 = \int \prod_{i\alpha\sigma} dc_{i\alpha\sigma}^\dagger dc_{i\alpha\sigma} \exp\left(-\sum_{i\alpha\sigma} c_{i\alpha\sigma}^\dagger c_{i\alpha\sigma}\right) |\{c_{i\alpha\sigma}\}\rangle \langle\{c_{i\alpha\sigma}\}|$,

where $\{c_{i\alpha\sigma}^\dagger, c_{i\alpha\sigma}\}$ denotes a set of Grassmann fields satisfying anti-periodic boundary conditions: $c_{i\alpha\sigma}^\dagger(0) = -c_{i\alpha\sigma}^\dagger(\beta)$ and $c_{i\alpha\sigma}(0) = -c_{i\alpha\sigma}(\beta)$; while the set of unit vectors defines the vector field $\{\mathbf{n}_{i\alpha}\}$, satisfying periodic ones: $\mathbf{n}_{i\alpha}(0) = \mathbf{n}_{i\alpha}(\beta)$, under a weight functional (see below). Thereby, following standard procedure [58, 59], the partition function reads:

$$\mathcal{Z} = \int \prod_{i\alpha\sigma} \mathcal{D}c_{i\alpha\sigma}^\dagger \mathcal{D}c_{i\alpha\sigma} \prod_{i\alpha} \mathcal{D}^2\mathbf{n}_{i\alpha} W(\{\mathbf{n}_{i\alpha}\}) e^{-\int_0^\beta \mathcal{L}(\tau) d\tau}, \quad (5)$$

where the pertinent measures are defined by

$$\mathcal{D}c_{i\alpha\sigma}^\dagger \mathcal{D}c_{i\alpha\sigma} \equiv \lim_{M \rightarrow \infty, \delta\tau \rightarrow 0} \prod_{r=1}^{M-1} dc_{i\alpha\sigma}^\dagger(\tau_r) dc_{i\alpha\sigma}(\tau_r), \quad (6)$$

$$\mathcal{D}^2\mathbf{n}_{i\alpha} \equiv \lim_{M \rightarrow \infty, \delta\tau \rightarrow 0} \prod_{r=1}^{M-1} d^2\mathbf{n}_{i\alpha}(\tau_r), \quad (7)$$

the weight functional, $W(\{\mathbf{n}_{i\alpha}\})$, satisfies a normalization condition at each discrete imaginary time τ_r :

$$\int \prod_{i\alpha} d^2\mathbf{n}_{i\alpha} W(\{\mathbf{n}_{i\alpha}(\tau_r)\}) = 1, \quad (8)$$

and the Lagrangian density $\mathcal{L}(\tau)$ is written in the form:

$$\begin{aligned} \mathcal{L}(\tau) = & \sum_{i\alpha\sigma} c_{i\alpha\sigma}^\dagger \partial_\tau c_{i\alpha\sigma} - \sum_{ij\alpha\beta\sigma} (t_{ij}^{\alpha\beta} c_{i\alpha\sigma}^\dagger c_{j\beta\sigma} + \text{H.c.}) \\ & + U \sum_{i\alpha} [\frac{\rho_{i\alpha}}{2} - 2(\mathbf{S}_{i\alpha} \cdot \mathbf{n}_{i\alpha})^2]. \end{aligned} \quad (9)$$

In order to fix $W(\{\mathbf{n}_{i\alpha}\})$ one should notice that, in the operator formalism: $\hat{\rho}_{i\alpha}^2 = \hat{\rho}_{i\alpha} + 2\hat{n}_{i\alpha\uparrow}\hat{n}_{i\alpha\downarrow}$. Therefore, using Eq. (2), the following identity holds [54]:

$$2(\hat{\mathbf{S}}_{i\alpha} \cdot \mathbf{n}_{i\alpha})^2 = \frac{\hat{\rho}_{i\alpha}(2 - \hat{\rho}_{i\alpha})}{2}, \quad (10)$$

which means that the square of the spin component operator along the $\mathbf{n}_{i\alpha}$ direction has zero eigenvalues if the site is vacant or doubly occupied, and a nonzero value only for singly occupied sites, i.e., $(\hat{\mathbf{S}}_{i\alpha} \cdot \mathbf{n}_{i\alpha})^2 = 1/4$. Now, taking advantage of the choice of $\mathbf{n}_{i\alpha}$, the local spin-polarization and spin-quantization axes are both chosen along the $\mathbf{n}_{i\alpha}$ direction. Therefore, for singly occupied sites, we find $\mathbf{S}_{i\alpha} \cdot \mathbf{n}_{i\alpha} = p_{i\alpha}/2$, with $p_{i\alpha} = \pm 1$, corresponding to the two possible spin-1/2 states. Further, by incorporating vacancy and double occupancy possibilities, corresponding to the four possible local states of the Hubbard model, one can write [54]

$$p_{i\alpha} \hat{\mathbf{S}}_{i\alpha} \cdot \mathbf{n}_{i\alpha} = \frac{\hat{\rho}_{i\alpha}(2 - \hat{\rho}_{i\alpha})}{2}, \quad (11)$$

with $p_{i\alpha}^2 = (\pm 1)^2$. We stress that, due to fermion operator properties, the square of Eq. (11) reproduces Eq. (10), and a comparison between them implies, at arbitrary doping and

U value, the formal equivalence between $2(\hat{\mathbf{S}}_{i\alpha} \cdot \mathbf{n}_{i\alpha})^2$ and $p_{i\alpha}(\hat{\mathbf{S}}_{i\alpha} \cdot \mathbf{n}_{i\alpha})$. In this context, we remark that the original Coulomb repulsion term of the Hubbard Hamiltonian in Eq. (1) is formally and energetically (eigenvalues) equivalent to both that in Eq. (9) or in its linear version through the following replacement: $2(\hat{\mathbf{S}}_{i\alpha} \cdot \mathbf{n}_{i\alpha})^2 \rightarrow p_{i\alpha}(\hat{\mathbf{S}}_{i\alpha} \cdot \mathbf{n}_{i\alpha})$. Indeed, using the constraint in Eq. (11) we find, $U \sum_{i\alpha} [\frac{\rho_{i\alpha}}{2} - p_{i\alpha}(\mathbf{S}_{i\alpha} \cdot \mathbf{n}_{i\alpha})] = U \sum_{i\alpha} [\frac{\rho_{i\alpha}}{2} - \frac{1}{2}\rho_{i\alpha}(2 - \rho_{i\alpha})]$, which is zero for $\rho_{i\alpha} = 0, 1$; whereas, as expected, for double occupied sites, $\rho_{i\alpha} = 2$, the local energy is U . Therefore, Eq. (11) in its Grassmann version, can be enforced by a proper choice of the normalized weight functional:

$$\begin{aligned} W(\{\mathbf{n}_{i\alpha}\}) &= \lim_{M \rightarrow \infty, \delta\tau \rightarrow 0} \prod_{r=1}^M W(\{\mathbf{n}_{i\alpha}(\tau_r)\}) \\ &= \mathcal{C} \exp \left\{ - \int_0^\beta d\tau \gamma \sum_{i\alpha} [p_{i\alpha} \mathbf{S}_{i\alpha} \cdot \mathbf{n}_{i\alpha} - \frac{\rho_{i\alpha}}{2}(2 - \rho_{i\alpha})]^2 \right\}, \end{aligned} \quad (12)$$

where $\gamma \rightarrow \infty$ in the continuum limit ($M \rightarrow \infty, \delta\tau \rightarrow 0$), with delta-function peaks at the four local states of the Hubbard model, and \mathcal{C} is a normalization factor such that Eq. (8) holds. In fact, the product of $W(\{\mathbf{n}_{i\alpha}(\tau_r)\})$ in Eq. (12) generates a sum in r in the exponential of the suitable chosen Gaussian function, i.e., $W(\{\mathbf{n}_{i\alpha}\})$ is such that in the continuum limit, $M \rightarrow \infty, \delta\tau \rightarrow 0$, Eq. (12) obtains with a diverging γ , as pointed out in Ref. [54]. In this way, using Eq. (12) for the weight functional in Eq. (5) for the partition function \mathcal{Z} , and integrating over $\{\mathbf{n}_{i\alpha}\}$, the Lagrangian density $\mathcal{L}(\tau)$ in Eq. (9) can thus be written in the following linearized form [54]:

$$\begin{aligned} \mathcal{L}(\tau) = & \sum_{i\alpha\sigma} c_{i\alpha\sigma}^\dagger \partial_\tau c_{i\alpha\sigma} - \sum_{ij\alpha\beta\sigma} (t_{ij}^{\alpha\beta} c_{i\alpha\sigma}^\dagger c_{j\beta\sigma} + \text{H.c.}) \\ & + U \sum_{i\alpha} [\frac{\rho_{i\alpha}}{2} - p_{i\alpha}(\mathbf{S}_{i\alpha} \cdot \mathbf{n}_{i\alpha})], \end{aligned} \quad (13)$$

where the constraint in Eq. (11) was explicitly used.

Now, since we are interested in studying the GS properties of the AB_2 Hubbard chains, we choose the staggered factor $p_{i\alpha} = +1$ (-1) at sites $\alpha = B_1$, B_2 (A), consistent with the long-range ferrimagnetic GS predicted by Lieb's theorem at half filling and for any U value [7, 8, 15], in which case we assume broken rotational symmetry along the z -axis. In this context, by considering the symmetry exhibited by the ferrimagnetic order, let us define the $SU(2)/U(1)$ unitary rotation matrix [60]

$$U_{i\alpha} = \begin{bmatrix} \cos\left(\frac{\theta_{i\alpha}}{2}\right) & -\sin\left(\frac{\theta_{i\alpha}}{2}\right) e^{-i\phi_{i\alpha}} \\ \sin\left(\frac{\theta_{i\alpha}}{2}\right) e^{i\phi_{i\alpha}} & \cos\left(\frac{\theta_{i\alpha}}{2}\right) \end{bmatrix}, \quad (14)$$

where $\theta_{i\alpha}$ is the polar angle between the z -axis and the unit local vector $\mathbf{n}_{i\alpha}$ and $\phi_{i\alpha} \in [0, 2\pi)$ is an arbitrary azimuth angle due to the $U(1)$ gauge freedom of choice for $U_{i\alpha}$. Moreover, a new set of Grassmann fields, $\{a_{i\alpha\sigma}^\dagger, a_{i\alpha\sigma}\}$ can be obtained, according to the transformation:

$$c_{i\alpha\sigma} = \sum_{\sigma'} (U_{i\alpha})_{\sigma\sigma'} a_{i\alpha\sigma'}, \quad (15)$$

that locally rotates each unit vector $\mathbf{n}_{i\alpha}$ to the z -direction. On the other hand, if we express the product $\boldsymbol{\sigma} \cdot \mathbf{n}_{i\alpha}$ in matrix form:

$$\boldsymbol{\sigma} \cdot \mathbf{n}_{i\alpha} = \begin{bmatrix} \cos(\theta_{i\alpha}) & \sin(\theta_{i\alpha}) e^{-i\phi_{i\alpha}} \\ \sin(\theta_{i\alpha}) e^{i\phi_{i\alpha}} & -\cos(\theta_{i\alpha}) \end{bmatrix}, \quad (16)$$

we obtain, after using Eq. (14),

$$U_{i\alpha}^\dagger (\boldsymbol{\sigma} \cdot \mathbf{n}_{i\alpha}) U_{i\alpha} = \sigma^z, \quad (17)$$

which explicitly manifest the broken rotational symmetry along the z -axis. In this way, by substituting Eqs. (14) and (15) into Eq. (3), and using the above result, we find

$$\begin{aligned} \mathbf{S}_{i\alpha} \cdot \mathbf{n}_{i\alpha} &= \frac{1}{2} \sum_{\sigma\sigma'} a_{i\alpha\sigma}^\dagger [U_{i\alpha}^\dagger (\boldsymbol{\sigma} \cdot \mathbf{n}_{i\alpha}) U_{i\alpha}]_{\sigma\sigma'} a_{i\alpha\sigma'} \\ &= \frac{1}{2} \sum_{\sigma\sigma'} a_{i\alpha\sigma}^\dagger (\sigma_z)_{\sigma\sigma'} a_{i\alpha\sigma'} \equiv S_{i\alpha}^z; \end{aligned} \quad (18)$$

thereby, the constraint in Eq. (11) can be written in the form

$$\mathbf{S}_{i\alpha} \cdot \mathbf{n}_{i\alpha} = p_{i\alpha} \frac{\rho_{i\alpha}(2 - \rho_{i\alpha})}{2} = \frac{1}{2} (a_{i\alpha\uparrow}^\dagger a_{i\alpha\uparrow} - a_{i\alpha\downarrow}^\dagger a_{i\alpha\downarrow}), \quad (19)$$

where $p_{i\alpha} = +1$ (-1) at sites $\alpha = B_1, B_2$ (A). The choice of $p_{i\alpha}$ above implies Lieb's ferrimagnetic ordering with the set $\{\theta_{iA} = \theta_{iB_1} = \theta_{iB_2} = 0\}$, for all i , at half filling. However, in the hole doped regime away from half filling, the $\theta_{i\alpha}$'s can be nonzero (e.g., $\theta_{i\alpha} = \pi$ for a spin flip, leading to a change in the sign of $S_{i\alpha}^z$); further, $S_{i\alpha}^z$ can be zero either by the presence of holes or doubly occupied sites ($a_{i\alpha\uparrow}^\dagger a_{i\alpha\uparrow} = a_{i\alpha\downarrow}^\dagger a_{i\alpha\downarrow}$). Lastly, using Eqs. (15) and (19) into the Lagrangian, Eq. (13), we find, after suitable rearrangement of terms,

$$\mathcal{L}(\tau) = \mathcal{L}_0(\tau) + \mathcal{L}_n(\tau), \quad (20)$$

where both Lagrangians are quadratic in the Grassmann fields:

$$\begin{aligned} \mathcal{L}_0(\tau) &= \sum_{i\alpha\sigma} a_{i\alpha\sigma}^\dagger \partial_\tau a_{i\alpha\sigma} - \sum_{i\alpha j\beta\sigma} (t_{ij}^{\alpha\beta} a_{i\alpha\sigma}^\dagger a_{j\beta\sigma} + \text{H.c.}) \\ &\quad + \frac{U}{2} \sum_{i\alpha\sigma} (1 - p_{i\alpha}\sigma) a_{i\alpha\sigma}^\dagger a_{i\alpha\sigma}, \end{aligned} \quad (21)$$

and

$$\begin{aligned} \mathcal{L}_n(\tau) &= \sum_{i\alpha\sigma\sigma'} a_{i\alpha\sigma'}^\dagger (U_{i\alpha}^\dagger \partial_\tau U_{i\alpha})_{\sigma'\sigma} a_{i\alpha\sigma} \\ &\quad - \sum_{i\alpha j\beta\sigma\sigma'} t_{ij}^{\alpha\beta} [a_{i\alpha\sigma'}^\dagger (U_{i\alpha}^\dagger U_{j\beta} - 1)_{\sigma'\sigma} a_{j\beta\sigma} + \text{H.c.}], \end{aligned} \quad (22)$$

with the first term in both Eqs. (21) and (22) being originated from the first term in Eq. (13), the second ones come from the hopping term in Eq. (13), after a rearrangement of terms, while the last one in Eq. (21) (proportional to U) is obtained by using Eq. (19) in the last term of Eq. (13). It is worth mentioning that only charge degrees of freedom (Grassmann fields) appear in $\mathcal{L}_0(\tau)$, and spin degrees of freedom under the

constraint in Eq. (19) [$SU(2)$ gauge fields $\{U_{i\alpha}^\dagger, U_{i\alpha}\}$, which carry all the information on the vector field $\{\mathbf{n}_{i\alpha}\}$] are now restricted to $\mathcal{L}_n(\tau)$, which includes both spin and charge degrees of freedom.

In the large- U regime, double occupancy is energetically unfavorable and the factor $2 - \rho_{i\alpha}$ is no longer needed in Eq. (19), i.e., $\mathbf{S}_{i\alpha} \cdot \mathbf{n}_{i\alpha} = p_{i\alpha} \frac{\rho_{i\alpha}}{2}$, with $\rho_{i\alpha} = 0$ or 1 . In this case, a proper perturbative analysis will allow us to study hole doping effects in Sec. V in a macroscopic fashion, so we define

$$\delta = 1 - \frac{1}{N} \sum_{i\alpha} \langle \rho_{i\alpha} \rangle, \quad (23)$$

which measures the thermodynamic average of hole doping away from half filling. In this context (strong-coupling limit), we take advantage of results derived from $\mathcal{L}_0(\tau)$ (charge effects in Sec. III), and at half filling (Sec. IV), in which case charge degrees of freedom are frozen.

III. CHARGE DEGREES OF FREEDOM AND THE STRONG-COUPLING LIMIT

In this section, we shall first diagonalize the Hamiltonian associated with the Lagrangian $\mathcal{L}_0(\tau)$ through the use of a special symmetry property of the AB_2 chains and a canonical transformation in reciprocal space. Then, by introducing a perturbative expansion in the strong-coupling regime, a low-energy effective Lagrangian for the AB_2 Hubbard chains at half filling and in the doped regime will be obtained.

A. Charge degrees of freedom

We begin our discussion by considering the Lagrangian \mathcal{L}_0 in Eq. (21), and its corresponding Hamiltonian \mathcal{H}_0 , free of the $SU(2)$ gauge fields. By performing the Legendre transformation: $\mathcal{H}_0 = -\sum_{i\alpha\sigma} \frac{\partial \mathcal{L}_0}{\partial (\partial_\tau a_{i\alpha\sigma})} \partial_\tau a_{i\alpha\sigma} + \mathcal{L}_0$, where $\frac{\partial \mathcal{L}_0}{\partial (\partial_\tau a_{i\alpha\sigma})} = a_{i\alpha\sigma}^\dagger$, the resulting \mathcal{H}_0 is given by

$$\begin{aligned} \mathcal{H}_0 &= - \sum_{\langle i\alpha, j\beta \rangle \sigma} (t_{ij}^{\alpha\beta} a_{i\alpha\sigma}^\dagger a_{j\beta\sigma} + \text{H.c.}) \\ &\quad + \frac{U}{2} \sum_{i\alpha\sigma} (1 - p_{i\alpha}\sigma) a_{i\alpha\sigma}^\dagger a_{i\alpha\sigma}. \end{aligned} \quad (24)$$

Further, since \mathcal{H}_0 (\mathcal{L}_0) is quadratic in the Grassmann fields, the solution for the energy of the system is given by \mathcal{H}_0 in its diagonalized form [59].

The AB_2 unit cell topology exhibits a symmetry [9, 11, 24, 25, 55] under the exchange of the labels of the B sites in a given unit cell. Thus, we can construct a new set of Grassmann fields possessing this symmetry, i.e., either symmetric or antisymmetric with respect to the exchange operation $B_1 \leftrightarrow B_2$:

$$(d_{i\sigma}, e_{i\sigma}) = \frac{1}{\sqrt{2}} (a_{iB_1\sigma} \pm a_{iB_2\sigma}), \quad b_{i\sigma} = a_{iA\sigma}. \quad (25)$$

In addition, as a signature of the quasi-1D structure of the AB_2 chains, we notice that the B_1 and B_2 sites are located at a distance $1/2$ (in units of length) ahead of the A site. Therefore, after Fourier transforming the above Grassmann fields, i.e., $\{d_{i,\sigma}, e_{i,\sigma}, b_{i,\sigma}\} = \frac{1}{\sqrt{N_c}} \sum_k e^{ikx_i} \{d_{k,\sigma}, e_{k,\sigma}, b_{k,\sigma}\}$, it is convenient to introduce a phase factor $e^{\frac{ik}{2}}$ through the following transformation [55]: $(A_{k\sigma}, B_{k\sigma}) = \frac{1}{\sqrt{2}}(d_{k\sigma} \pm e^{\frac{ik}{2}} b_{k\sigma})$, so that \mathcal{H}_0 in Eq. (24) thus becomes

$$\begin{aligned} \mathcal{H}_0 = & \sum_{k\sigma} \varepsilon_k [A_{k\sigma}^\dagger A_{k\sigma} - B_{k\sigma}^\dagger B_{k\sigma}] + \frac{U}{2} \sum_{k\sigma} (1 - \sigma) e_{k\sigma}^\dagger e_{k\sigma} \\ & + \frac{U}{2} \sum_{k\sigma} [A_{k\sigma}^\dagger A_{k\sigma} + B_{k\sigma}^\dagger B_{k\sigma} - \sigma (A_{k\sigma}^\dagger B_{k\sigma} + B_{k\sigma}^\dagger A_{k\sigma})], \end{aligned} \quad (26)$$

where

$$\varepsilon_k = -2\sqrt{2}t \cos(k/2), \quad (27)$$

with $k = 2\pi j(\frac{3}{N}) - \pi$, and $j = 1, \dots, N/3$. We can now exactly diagonalize \mathcal{H}_0 through the following Bogoliubov transformation:

$$A_{k\sigma} = u_k \alpha_{k\sigma} - \sigma v_k \beta_{k\sigma}, \quad B_{k\sigma} = \sigma v_k \alpha_{k\sigma} + u_k \beta_{k\sigma}, \quad (28)$$

with u_k and v_k satisfying the canonical constraint: $(u_k)^2 + (v_k)^2 = 1$, to maintain the anticommutation relations of the Grassmann fields. Due to the ferrimagnetic order of the GS, the above transformation is subject to a 4π periodicity of the Bogoliubov functions $\{u_k, v_k\}$ and Grassmann fields $\{\alpha_{k\sigma}, \beta_{k\sigma}\}$. The diagonalized \mathcal{H}_0 thus reads:

$$\begin{aligned} \mathcal{H}_0 = & - \sum_{k\sigma} (E_k - \frac{U}{2}) \alpha_{k\sigma}^\dagger \alpha_{k\sigma} + \sum_{k\sigma} (E_k + \frac{U}{2}) \beta_{k\sigma}^\dagger \beta_{k\sigma} \\ & + \frac{U}{2} \sum_{k\sigma} (1 - \sigma) e_{k\sigma}^\dagger e_{k\sigma}, \end{aligned} \quad (29)$$

where

$$(u_k, v_k) = \frac{1}{\sqrt{2}} \left(1 \pm \frac{|\varepsilon_k|}{E_k} \right)^{1/2}, \quad (30)$$

and

$$E_k = \sqrt{\varepsilon_k^2 + U^2/4}. \quad (31)$$

As one can see from Eq. (29), the non-interacting tight binding ($U = 0$) spectrum of \mathcal{H}_0 present three electronic bands: a nondispersive flat band (related to the Grassmann fields $\{e_{k\sigma}^\dagger, e_{k\sigma}\}$, macroscopically degenerate), and two dispersive ones. In AB_2 chains, flat bands are closely associated with ferrimagnetism (unsaturated ferromagnetism) [5, 7, 8] at half filling, in agreement with Lieb's theorem [15, 16], or fully polarized ferromagnetism [17] associated with the flat lowest band. We also stress that even at this level of approximation and in the weak coupling regime ($U = 2t$), it was shown [7] that hole doping [parametrized by δ defined in Eq. (23)] can

destroy the ferrimagnetic order and/or induce phase separation in AB_2 chains. As depicted in Fig. 1(a), the $U = 0$ spin degeneracy of the flat bands is removed by the Coulombian repulsive interaction, in which case a gap U opens between the $e_{k\sigma}$ modes: $e_{k\uparrow} = 0$, where spins at sites B_1 and B_2 are up, and $e_{k\downarrow} = U$, where these spins are down. On the other hand, the two dispersive bands are spin degenerated, and also display a Hubbard gap U separating the low ($\alpha_{k\sigma}$)-energy and high ($\beta_{k\sigma}$)-energy modes [55].

B. Strong-coupling limit

In this subsection, we shall introduce a perturbative expansion in the strong-coupling regime ($U \gg t$) in order to obtain a low-energy effective Lagrangian for the AB_2 Hubbard chain at half filling and in the doped regime. First, we resume the results of the previous section by writing the Grassmann fields $d_{i\sigma}$ and $b_{i\sigma}$ in terms of the Grassmann (Bogoliubov) fields $\alpha_{k\sigma}$ and $\beta_{k\sigma}$:

$$\begin{aligned} (d_{i\sigma}, b_{i\sigma}) = & \frac{1}{\sqrt{2N_c}} \sum_k (e^{ikx_i}, e^{ik(x_i - \frac{1}{2})}) \\ & \times [(u_k \pm \sigma v_k) \alpha_{k\sigma} \pm (u_k \mp \sigma v_k) \beta_{k\sigma}], \end{aligned} \quad (32)$$

where the phase factor $e^{-\frac{ik}{2}}$ signalizes the quasi-1D AB_2 structure, and the antisymmetric Grassmann field $e_{i,\sigma}$ remains as defined in Eq. (25). In the strong-coupling limit, however, it will prove useful to define a set of auxiliary spinless Grassmann fields [54, 55] in direct space associated with $d_{i\sigma}$ and $b_{i\sigma}$:

$$(\alpha_i, \beta_i) = \sqrt{\frac{1}{N_c}} \sum_{k,\sigma} \theta(\pm\sigma) e^{ikx_i} (\alpha_{k\sigma}, \beta_{k\sigma}), \quad (33)$$

and a similar equation for $(\alpha_i^{\frac{1}{2}}, \beta_i^{\frac{1}{2}}) \leftrightarrow (\alpha_{k\sigma}, \beta_{k\sigma})$ is obtained by the replacements: $\theta(\pm\sigma) \rightarrow \theta(\mp\sigma)$ and $x_i \rightarrow x_i - 1/2$, where $\theta(\sigma)$ is the Heaviside function, while for the antisymmetric component, one has

$$e_{i,\sigma} = \sqrt{\frac{1}{N_c}} \sum_k e^{ikx_i} e_{k,\sigma}. \quad (34)$$

Now, by expanding (u_k, v_k) in Eq. (30) in powers of t/U :

$$(u_k, v_k) \approx \frac{1}{\sqrt{2}} \left[1 \pm \frac{|\varepsilon_k|}{U} + \mathcal{O}\left(\frac{t^2}{U^2}\right) \right], \quad (35)$$

substituting these results into the Eq. (32), and using the inverse transformation of Eq. (33), we can derive a perturbative expansion in powers of t/U for the Grassmann fields $d_{i\sigma}$ and $b_{i\sigma}$ in terms of the spinless Grassmann fields as follows:

$$\begin{aligned} d_{i\sigma} = & \theta(\sigma) \alpha_i + \theta(-\sigma) \beta_i + \sqrt{2} \frac{t}{U} \theta(-\sigma) (\alpha_i^{\frac{1}{2}} + \alpha_{i+1}^{\frac{1}{2}}) \\ & + \frac{t}{U} \theta(\sigma) [\sqrt{2} (\beta_i^{\frac{1}{2}} + \beta_{i+1}^{\frac{1}{2}}) - \frac{t}{U} (2\alpha_i + \alpha_{i+1} + \alpha_{i-1})] \\ & + \mathcal{O}(t^2/U^2), \end{aligned} \quad (36)$$

$$\begin{aligned}
b_{i\sigma} = & \theta(-\sigma)\alpha_i^{\frac{1}{2}} - \theta(\sigma)\beta_i^{\frac{1}{2}} + \sqrt{2}\frac{t}{U}\theta(\sigma)(\alpha_i + \alpha_{i-1}) \\
& - \frac{t}{U}\theta(-\sigma)[\sqrt{2}(\beta_i + \beta_{i-1}) + \frac{t}{U}(2\alpha_i^{\frac{1}{2}} + \alpha_{i+1}^{\frac{1}{2}} + \alpha_{i-1}^{\frac{1}{2}})] \\
& + \mathcal{O}(t^2/U^2). \quad (37)
\end{aligned}$$

In the above derivation, we have used that $\theta(\sigma)\theta(\sigma') = \theta(\sigma)\delta_{\sigma,\sigma'}$. Notice that, since $\frac{t}{U} \ll 1$, in Eqs. (36) and (37) we can identify the fields $\alpha_i^{\frac{1}{2}} \approx a_{iA\downarrow}$ and $\alpha_i \approx (a_{iB_1\uparrow} + a_{iB_2\uparrow})/\sqrt{2}$, a result fully consistent with the low-energy spin configuration of the ferrimagnetic state discussed previously. Analogously, for the high-energy bands, the opposite spin configuration is observed, with spin up (down) present at sites A (B_1, B_2).

Introducing Eqs. (36) and (37) into Eq. (24), with the aid of Eq. (25), we obtain a perturbative expression for \mathcal{H}_0 (low-energy sector) in terms of the spinless Grassmann fields up to order $J = 4t^2/U$:

$$\begin{aligned}
\mathcal{H}_0 = & -J \sum_i [\alpha_i^\dagger \alpha_i + \alpha_i^{(\frac{1}{2})\dagger} \alpha_i^{\frac{1}{2}} - \beta_i^\dagger \beta_i - \beta_i^{(\frac{1}{2})\dagger} \beta_i^{\frac{1}{2}}] \\
& - \frac{J}{2} \sum_i [\alpha_i^\dagger \alpha_{i+1} + \alpha_i^{(\frac{1}{2})\dagger} \alpha_{i+1}^{\frac{1}{2}} - \beta_i^\dagger \beta_{i+1} - \beta_i^{(\frac{1}{2})\dagger} \beta_{i+1}^{\frac{1}{2}} + \text{H.c.}] \\
& + U \sum_i [\beta_i^\dagger \beta_i + \beta_i^{(\frac{1}{2})\dagger} \beta_i^{\frac{1}{2}} + e_{i\downarrow}^\dagger e_{i\downarrow}]. \quad (38)
\end{aligned}$$

By applying Fourier transform to the above expression and rearranging the terms, we obtain

$$\begin{aligned}
\mathcal{H}_0 = & - \sum_k 2J \cos^2(k/2) (\alpha_k^\dagger \alpha_k + \alpha_k^{(\frac{1}{2})\dagger} \alpha_k^{\frac{1}{2}}) \\
& + \sum_k [2J \cos^2(k/2) + U] (\beta_k^\dagger \beta_k + \beta_k^{(\frac{1}{2})\dagger} \beta_k^{\frac{1}{2}}) \\
& + \frac{U}{2} \sum_{k\sigma} (1 - \sigma) e_{k\sigma}^\dagger e_{k\sigma}. \quad (39)
\end{aligned}$$

In Fig. 1 we plot the electronic spectrum of the Hamiltonian \mathcal{H}_0 , both in the weak and strong-coupling regime: (a) Eq. (29) for $U = 2t$ and (b) Eqs. (29) and (39) for $U = 12t$ ($J = 4t^2/U = 1/3$), respectively, with $t \equiv 1$. We can notice the presence of the shrinking phenomenon [7] as U increases from $2t$ to $12t$ (strong-coupling regime) and that, for $U = 12t$, Eq. (39) is a very good approximation to Eq. (29). Noticeably, the $t \ll U$ expansion of the fields allow us to identify $\alpha_k^{\frac{1}{2}} \approx a_{kA\downarrow}$, $\alpha_k \approx (a_{kB_1\uparrow} + a_{kB_2\uparrow})/\sqrt{2}$ (triplet state) and $e_{k\uparrow} \approx (a_{kB_1\uparrow} - a_{kB_2\uparrow})/\sqrt{2}$ (singlet state), as the low-energy spin configuration of the ferrimagnetic state with single occupancy, where spins at sites A (B_1, B_2) are down (up), in agreement with Lieb's theorem [7, 8, 15].

In order to describe the most relevant low-energy processes that take place in this regime, one has to additionally project out the high-energy bands from \mathcal{H}_0 , that is, terms containing only fields related to the high-energy bands are excluded. Therefore, after the Legendre transformation, $\mathcal{H}_0 = - \sum_{i,\eta_i} \frac{\partial \mathcal{L}_0}{\partial (\partial_\tau \eta_i)} \partial_\tau \eta_i + \mathcal{L}_0$, where $\eta_i = \alpha_i, \alpha_i^{\frac{1}{2}}$, and $e_{i\uparrow}$ (fields

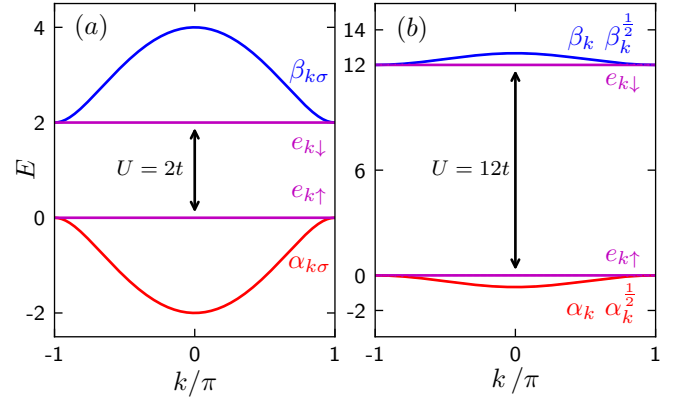


Figure 1. (Color online) Electronic spectrum of the Hamiltonian \mathcal{H}_0 : (a) Eq. (29) for $U = 2t$ and (b) Eqs. (29) and (39) for $U = 12t$ ($J = 4t^2/U = 1/3$), with $t \equiv 1$. Notice the band shrinking phenomenon as U increases from $2t$ to $12t$ (strong-coupling regime). The $t \ll U$ expansion of the fields identifies $\alpha_k^{\frac{1}{2}} \approx a_{kA\downarrow}$, $\alpha_k \approx (a_{kB_1\uparrow} + a_{kB_2\uparrow})/\sqrt{2}$ and $e_{k\uparrow} \approx (a_{kB_1\uparrow} - a_{kB_2\uparrow})/\sqrt{2}$, where spins at sites A (B_1, B_2) are down (up), in agreement with Lieb's theorem [15].

related to the low-energy bands), with $\frac{\partial \mathcal{L}_0}{\partial (\partial_\tau \eta_i)} = \eta_i^\dagger$, the Lagrangian associated with \mathcal{H}_0 (up to order J) is given by

$$\begin{aligned}
\mathcal{L}_0 = & \sum_{i,\eta_i} \eta_i^\dagger \partial_\tau \eta_i - J \sum_i (\alpha_i^\dagger \alpha_i + \alpha_i^{(\frac{1}{2})\dagger} \alpha_i^{\frac{1}{2}}) \\
& - \frac{J}{2} \sum_i (\alpha_i^\dagger \alpha_{i+1} + \alpha_i^{(\frac{1}{2})\dagger} \alpha_{i+1}^{\frac{1}{2}} + \text{H.c.}). \quad (40)
\end{aligned}$$

We shall now focus on the $U \gg t$ perturbative expansion of \mathcal{L}_n , Eq. (22), which amounts to consider the most significant low-energy processes, after the use of Eqs. (36) and (37) for $d_{i\sigma}$ and $b_{i\sigma}$ in terms of the spinless Grassmann fields. However, terms allowing interband transitions between low- and high-energy bands do exist in \mathcal{L}_n . In this context, we apply a suitable second-order Rayleigh-Schrödinger perturbation theory [54, 55], consistent with the strong-coupling expansion, so that the modes associated with the high-energy bands are eliminated. Lastly, by adding \mathcal{L}_0 to the perturbative expansion of \mathcal{L}_n , which leads to the cancellation of the exchange terms in Eq. (40), the effective low-energy Lagrangian density of the AB_2 Hubbard model in the strong-coupling limit (up to order J) reads:

$$\mathcal{L}_{eff}(\tau) = \mathcal{L}^{(I)} + \mathcal{L}^{(II)} + \mathcal{L}^{(III)} + \mathcal{L}^{(IV)}, \quad (41)$$

where

$$\mathcal{L}^{(I)} = \sum_i \alpha_i^\dagger \partial_\tau \alpha_i + \sum_i \alpha_i^{(\frac{1}{2})\dagger} \partial_\tau \alpha_i^{(\frac{1}{2})} + \sum_i e_{i\uparrow}^\dagger \partial_\tau e_{i\uparrow}, \quad (42a)$$

$$\begin{aligned} \mathcal{L}^{(II)} = & \sum_{i\sigma} \left\{ \theta(-\sigma) (U_i^{(b)\dagger} \partial_\tau U_i^{(b)})_{\sigma,\sigma} \alpha_i^{(\frac{1}{2})\dagger} \alpha_i^{(\frac{1}{2})} \right. \\ & + \theta(\sigma) \frac{1}{2} [(U_i^{(d)\dagger} \partial_\tau U_i^{(d)})_{\sigma,\sigma} + (U_i^{(e)\dagger} \partial_\tau U_i^{(e)})_{\sigma,\sigma}] \\ & \times (\alpha_i^\dagger \alpha_i + e_{i\uparrow}^\dagger e_{i\uparrow}) + \left[\theta(\sigma) \frac{1}{2} [(U_i^{(d)\dagger} \partial_\tau U_i^{(e)})_{\sigma,\sigma} \right. \\ & \left. \left. + (U_i^{(e)\dagger} \partial_\tau U_i^{(d)})_{\sigma,\sigma}] \alpha_i^\dagger e_{i\uparrow} + \text{H.c.} \right] \right\}, \quad (42b) \end{aligned}$$

$$\begin{aligned} \mathcal{L}^{(III)} = & -t \sum_{i\sigma} \left\{ \theta(-\sigma) (U_i^{(b)\dagger} U_i^{(d)})_{\sigma,-\sigma} \alpha_i^{(\frac{1}{2})\dagger} \alpha_i \right. \\ & + \theta(\sigma) (U_i^{(d)\dagger} U_{i+1}^{(b)})_{\sigma,-\sigma} \alpha_i^\dagger \alpha_{i+1}^{(\frac{1}{2})} \\ & + \theta(-\sigma) (U_i^{(b)\dagger} U_i^{(e)})_{\sigma,-\sigma} \alpha_i^{(\frac{1}{2})\dagger} e_{i\uparrow} \\ & \left. + \theta(\sigma) (U_i^{(e)\dagger} U_{i+1}^{(b)})_{\sigma,-\sigma} e_{i\uparrow}^\dagger \alpha_{i+1}^{(\frac{1}{2})} + \text{H.c.} \right\}, \quad (42c) \end{aligned}$$

$$\begin{aligned} \mathcal{L}^{(IV)} = & -\frac{J}{4} \sum_{i,i'=i,i+1;\sigma} \theta(\sigma) |(U_i^{(d)\dagger} U_{i'}^{(b)})_{\sigma,\sigma}|^2 \alpha_i^\dagger \alpha_i \\ & - \frac{J}{4} \sum_{i,i'=i,i+1;\sigma} \theta(\sigma) |(U_i^{(e)\dagger} U_{i'}^{(b)})_{\sigma,\sigma}|^2 e_{i\uparrow}^\dagger e_{i\uparrow} \\ & - \frac{J}{4} \sum_{i,i'=i,i-1;\sigma} \theta(-\sigma) |(U_i^{(b)\dagger} U_{i'}^{(d)})_{\sigma,\sigma}|^2 \\ & + (U_i^{(b)\dagger} U_{i'}^{(e)})_{\sigma,\sigma}|^2 \alpha_i^{(\frac{1}{2})\dagger} \alpha_i^{(\frac{1}{2})}, \quad (42d) \end{aligned}$$

where

$$U_i^{(b)} = U_{iA}, \quad U_i^{(d,e)} = \frac{1}{\sqrt{2}} (U_{iB_1} \pm U_{iB_2}), \quad (43)$$

in which case we took advantage of the symmetry of the AB_2 chain under the exchange operation $B_1 \leftrightarrow B_2$, in correspondence with Eq. (25). From the above equations, we see that the kinetic term is represented by $\mathcal{L}^{(I)}$ and is related to the charge degrees of freedom only, whereas $\mathcal{L}^{(II)}$ describes the dynamics of the spin degrees of freedom coupled to the charge fields. On the other hand, $\mathcal{L}^{(III)}$ exhibit first-neighbor hopping contributions between charge degrees of freedom in the presence of $SU(2)$ gauge fields, while $\mathcal{L}^{(IV)}$ is the spin exchange term in the presence of the charge Grassmann fields.

IV. HALF-FILLING REGIME

Let us now discuss some basic aspects of the localized magnetic properties related to the spin degrees of freedom. At half filling, i.e., $\delta = 0$, we have $\langle \alpha_i^\dagger \alpha_i \rangle = 1$, $\langle \alpha_i^{(1/2)\dagger} \alpha_i^{(1/2)} \rangle = 1$, $\langle e_{i\uparrow}^\dagger e_{i\uparrow} \rangle = 1$, and $\langle \alpha_i^\dagger e_{i\uparrow} \rangle = 0$ (no band hybridization) as the electrons tend to fill up the lower-energy bands, whereas the higher-energy ones remain empty. As a consequence, a ferromagnetic configuration of localized spins emerges, i.e., the charge degrees of freedom are completely frozen, such that $\langle \alpha_i^\dagger \partial_\tau \alpha_i \rangle = \langle \alpha_i^{(1/2)\dagger} \partial_\tau \alpha_i^{(1/2)} \rangle = \langle e_{i\uparrow}^\dagger \partial_\tau e_{i\uparrow} \rangle = 0$, with forbidden hopping. Therefore, only terms from $\mathcal{L}^{(II)}$ and $\mathcal{L}^{(IV)}$ in

Eqs. (42b) and (42d), respectively, give nonzero contributions and the resulting effective strong-coupling Lagrangian at half filling, defined in Eq. (41), reads:

$$\begin{aligned} \mathcal{L}_{eff}^J = & \sum_{i\alpha\sigma} \theta(p_{i\alpha}\sigma) (U_{i\alpha}^\dagger \partial_\tau U_{i\alpha})_{\sigma,\sigma} \\ & - \frac{J}{4} \sum_{\langle i\alpha,j\beta \rangle \sigma} \theta(p_{i\alpha}\sigma) \left| (U_{i\alpha}^\dagger U_{j\beta})_{\sigma,\sigma} \right|^2, \quad (44) \end{aligned}$$

where the staggered factor $p_{i\alpha}$ was defined in Eq. (11), and use was made of the matrix transformations defined in Eq. (43) in order to sum up the squares of the $SU(2)$ gauge field products in the exchange contribution from $\mathcal{L}^{(IV)}$ in Eq. (42d). Now, using the following Legendre transform: $\mathcal{H}_{eff}^J = -\sum_{i\alpha\sigma} \frac{\partial \mathcal{L}_{eff}^J}{\partial (\partial_\tau U_{i\alpha})_{\sigma,\sigma}} (\partial_\tau U_{i\alpha})_{\sigma,\sigma} + \mathcal{L}_{eff}^J$, where $\frac{\partial \mathcal{L}_{eff}^J}{\partial (\partial_\tau U_{i\alpha})_{\sigma,\sigma}} = \theta(p_{i\alpha}\sigma) (U_{i\alpha}^\dagger)_{\sigma,\sigma}$, we get the respective quantum Heisenberg Hamiltonian written in terms of the $SU(2)$ gauge fields at half filling as

$$\mathcal{H}_{eff}^J = -\frac{J}{4} \sum_{\langle i\alpha,j\beta \rangle \sigma} \theta(p_{i\alpha}\sigma) \left| (U_{i\alpha}^\dagger U_{j\beta})_{\sigma,\sigma} \right|^2. \quad (45)$$

Further, using the definition of the $SU(2)/U(1)$ unitary rotation matrix Eq. (14), it is possible to write [54–56] $\left| (U_{i\alpha}^\dagger U_{j\beta})_{\sigma,\sigma} \right|^2 = \frac{1}{2} (1 + \mathbf{n}_{i\alpha} \cdot \mathbf{n}_{j\beta})$, where $\mathbf{n}_{i\alpha} = \sin(\theta_{i\alpha}) [\cos(\phi_{i\alpha}) \hat{\mathbf{x}} + \sin(\phi_{i\alpha}) \hat{\mathbf{y}}] + \cos(\theta_{i\alpha}) \hat{\mathbf{z}}$ is the unit vector pointing along the local spin direction. Lastly, by using the constraint as given in Eq. (19), we can identify the spin field $\{\mathbf{S}_{i\alpha}\}$ at the single occupied sites:

$$\mathbf{S}_{i\alpha} = p_{i\alpha} \mathbf{n}_{i\alpha} / 2, \quad (46)$$

where $p_{i\alpha} = +1$ (-1) at sites $\alpha = B_1, B_2$ (A), in order to obtain

$$\mathcal{H}_{eff}^J = J \sum_i \left[(\mathbf{S}_i^{B_1} + \mathbf{S}_i^{B_2}) \cdot (\mathbf{S}_i^A + \mathbf{S}_{i+1}^A) \right] - J N_c. \quad (47)$$

The above expression is indeed that of the quantum antiferromagnetic Heisenberg spin-1/2 model on the AB_2 chain in zero-field, which takes into account the effects of zero-point quantum spin fluctuations. In fact, to achieve this goal, we analyze the Hamiltonian, Eq. (47), by means of the spin-wave theory, which has proved very successful in describing the properties of the GS and low-lying excited states of spin models. The predicted results provide a check of the consistency of our approach and will be fully used in our description of the doped regime.

We shall first introduce boson creation and annihilation operators via the Holstein-Primakoff [58] transformation:

$$\begin{aligned} S_i^{A,z} &= -S + a_i^\dagger a_i, \\ S_i^{A,+} &= (S_i^{A,-})^\dagger = \sqrt{2S} a_i^\dagger f_A(S), \end{aligned} \quad (48)$$

for a down-spin on the A site, and

$$\begin{aligned} S_i^{B_1,z} &= S - b_{li}^\dagger b_{li}, \\ S_i^{B_1,+} &= (S_i^{B_1,-})^\dagger = \sqrt{2S} f_B(S) b_{li}, \end{aligned} \quad (49)$$

for an up-spin on the B_l site, with $l = 1, 2$, and

$$f_r(S) = \left(1 - \frac{n_r}{2S}\right)^{1/2} = 1 - \frac{1}{2} \frac{n_r}{2S} + \dots, \quad (50)$$

where S is the spin magnitude, and $n_r = a_i^\dagger a_i$ or $b_{li}^\dagger b_{li}$. The operators a_i^\dagger and a_i (or b_{li}^\dagger , b_{li}) satisfy the boson commutation rules. Under the above transformation, the spin Hamiltonian, Eq. (47) is mapped onto the boson Hamiltonian:

$$\mathcal{H}_{eff}^J = E_0 - JN_c + \mathcal{H}_1 + \mathcal{H}_2 + \mathcal{O}(S^{-1}), \quad (51)$$

where

$$E_0 = -4S^2 JN_c, \quad (52)$$

is the classical GS energy and \mathcal{H}_1 and \mathcal{H}_2 are the quadratic and quartic (interacting) terms of the boson Hamiltonian, suitable to describe the quantum AB_2 Heisenberg model via a perturbative series expansion in powers of $1/S$. By Fourier transforming the boson operators, we find

$$\begin{aligned} \mathcal{H}_1 = & 2JS \sum_k (2a_k^\dagger a_k + \sum_l b_{lk}^\dagger b_{lk}) \\ & + \sum_{k,l=1,2} 2JS\gamma_k (a_k^\dagger b_{lk}^\dagger + a_k b_{lk}), \end{aligned} \quad (53)$$

where we have defined the lattice structure factor as

$$\gamma_k = \frac{1}{z} \sum_\rho e^{ik\rho} = \cos\left(\frac{k}{2}\right), \quad (54)$$

with z denoting the coordination number ($z = 4$ for the AB_2 chain), while $\rho = \pm 1/2$ connects the nearest neighbors A - B_1 and A - B_2 linked sites of sublattices A and B , and

$$\begin{aligned} \mathcal{H}_2 = & -\frac{3J}{2N} \sum_{1234, l=1,2} \delta_{12,34} \left\{ 4\gamma_{1-4} a_1^\dagger a_4 b_{l3}^\dagger b_{l2} \right. \\ & \left. + (\gamma_1 a_1^\dagger b_{l4}^\dagger b_{l3}^\dagger b_{l2} + \gamma_{1+2-3} a_1^\dagger a_2^\dagger a_3 b_{l4}^\dagger + \text{H.c.}) \right\}. \end{aligned} \quad (55)$$

For simplicity, we use the convention 1 for k_1 , 2 for k_2 , and so on. Also, the $\delta_{12,34} = \delta(k_1 + k_2 - k_3 - k_4)$ is the Kronecker δ function, and expresses the conservation of momentum to within a reciprocal-lattice vector G .

We shall consider \mathcal{H}_1 first, which is the term leading to linear spin-wave theory (LSWT). In fact, \mathcal{H}_1 is diagonalized using the following Bogoliubov transformation:

$$\begin{aligned} a_k &= u_k \beta_k - v_k \alpha_k^\dagger, \\ b_{lk} &= \frac{1}{\sqrt{2}} [u_k \alpha_k - v_k \beta_k^\dagger + (-1)^l \xi_k], \text{ with } l = 1, 2, \end{aligned} \quad (56)$$

$$(u_k, v_k) = \frac{(3 + \sqrt{9 - 8\gamma_k^2}, 2\sqrt{2}\gamma_k)}{\sqrt{(3 + \sqrt{9 - 8\gamma_k^2})^2 - 8\gamma_k^2}}, \quad (57)$$

where u_k and v_k satisfy the constraint $u_k^2 - v_k^2 = 1$. Thus,

$$\mathcal{H}_1 = E_1 + \sum_k (\epsilon_k^{(0(\alpha))} \alpha_k^\dagger \alpha_k + \epsilon_k^{(0(\beta))} \beta_k^\dagger \beta_k + \epsilon_k^{(0(\xi))} \xi_k^\dagger \xi_k); \quad (58)$$

$$E_1 = JS \sum_k (\sqrt{9 - 8\gamma_k^2} - 3), \quad (59)$$

$$\epsilon_k^{0(\alpha, \beta)} = JS(\sqrt{9 - 8\gamma_k^2} \mp 1), \quad \epsilon_k^{0(\xi)} = 2JS, \quad (60)$$

where E_1 is the $\mathcal{O}(S^1)$ quantum correction to the GS energy, and $\epsilon_k^{0(\alpha, \beta)}$, $\epsilon_k^{0(\xi)}$ are the three spin-wave branches provided by LSWT, both in agreement with previous results [19, 61]. In fact, it is well known that systems with a ferrimagnetic GS naturally have ferromagnetic and antiferromagnetic spin-wave modes as their elementary magnetic excitations (magnons). For the AB_2 chain, there are three spin-wave branches: an antiferromagnetic mode ($\epsilon_k^{0(\beta)}$) and two ferromagnetic ones ($\epsilon_k^{0(\alpha)}$ and $\epsilon_k^{0(\xi)}$). The mode $\epsilon_k^{0(\alpha)}$ is gapless at $k = 0$, i.e., the Goldstone mode, with a quadratic (ferromagnetic) dispersion relation $\epsilon_k^{0(\alpha)} \sim k^2$. The other two modes are gapped. Notice that the gapped ferromagnetic mode $\epsilon_k^{0(\xi)}$ is flat, and is closely associated with ferrimagnetic properties at half filling [7, 17]. Since the dispersive modes preserve the local triplet bond, they are identical to those found in the spin-1/2 - spin-1 chains [62–65]. These chains also exhibit interesting field-induced Luttinger liquid behavior [66].

Now, our aim is to obtain the leading corrections to LSWT, i.e., second-order spin-wave theory to the GS energy, sublattice magnetizations and Lieb GS total spin per unit cell. In doing so, we develop a perturbative scheme for the description of this quartic term. First, we decompose the two-body terms by means of the Wick theorem, via normal-ordering protocol for boson operators. Conservation of momentum to within a reciprocal-lattice vector, implies: $k_1 = k + q$, $k_2 = p - q$, $k_3 = k$ and $k_4 = p$. Then, we need to look at the possible pairings of the 4 operators, as for example, in the first term of Eq. (55):

$$a_{k+q}^\dagger a_p b_{l,k}^\dagger b_{l,p-q}, \quad a_{k+q}^\dagger a_p b_{l,k}^\dagger b_{l,p-q}, \quad a_{k+q}^\dagger a_p b_{l,k}^\dagger b_{l,p-q}.$$

Under this procedure, and by substituting the Bogoliubov transformation, Eqs. (56)-(57), into Eq. (55), we find

$$\mathcal{H}_2 = E_2 + \sum_k (\delta \epsilon_k^{(\alpha)} \alpha_k^\dagger \alpha_k + \delta \epsilon_k^{(\beta)} \beta_k^\dagger \beta_k + \delta \epsilon_k^{(\xi)} \xi_k^\dagger \xi_k), \quad (61)$$

where

$$E_2/N_c = -2J(q_1^2 + q_2^2 - \frac{3}{\sqrt{2}} q_1 q_2), \quad (62)$$

and the corresponding corrections for the spin-wave dispersion relations read:

$$\begin{aligned} \delta \epsilon_k^{(\alpha)} &= J[u_k^2(\sqrt{2}q_2 - 2q_1) + 2v_k^2(\sqrt{2}q_2 - q_1)] \\ &+ 4J\gamma_k u_k v_k \left[\frac{3}{2\sqrt{2}} q_1 - q_2 \right] + \mathcal{O}(S^{-1}), \end{aligned} \quad (63)$$

$\delta \epsilon_k^{(\beta)}$ is obtained from $\delta \epsilon_k^{(\alpha)}$ through the exchange of $u_k \leftrightarrow v_k$, and

$$\delta \epsilon_k^{(\xi)} = J(\sqrt{2}q_2 - 2q_1) + \mathcal{O}(S^{-1}). \quad (64)$$

In Eqs. (62)-(64) above, the quantities q_1 and q_2 are defined by (thermodynamic limit)

$$q_1 = \frac{1}{2\pi} \int_{-\pi}^{\pi} dk (v_k^2), \quad q_2 = \frac{1}{2\pi} \int_{-\pi}^{\pi} dk (\gamma_k u_k v_k). \quad (65)$$

We remark that in deriving Eqs. (62)-(64), we have neglected terms containing anomalous products, such as, $\alpha_k^\dagger \beta_k^\dagger$ and vertex corrections.

Lastly, the above results of our perturbative $1/S$ series expansion lead to the effective Hamiltonian:

$$\mathcal{H}_{eff}^J = E_{GS}^J - JN_c + \sum_k (\epsilon_k^\alpha \alpha_k^\dagger \alpha_k + \epsilon_k^{(\beta)} \beta_k^\dagger \beta_k + \epsilon_k^{(\xi)} \xi_k^\dagger \xi_k), \quad (66)$$

where

$$E_{GS}^J = E_0 + E_1 + E_2, \quad (67)$$

which can be read from Eqs. (52), (59), and (62), respectively, is the second-order result up to $\mathcal{O}(1/S)$ for the GS energy, and

$$\epsilon_k^{(s)} = \epsilon_k^{0(s)} + \delta\epsilon_k^{(s)}, \quad \text{with } s = \alpha, \beta, \xi, \quad (68)$$

are the corresponding second-order spin-wave modes, where the linear and the second-order correction terms are given by Eq. (60) and Eqs. (63)-(65), respectively.

A. Second-order spin-wave analysis

Our perturbative $1/S$ series expansion approach is able to improve the LSWT result for the gap $\Delta = J$ of the antiferromagnetic mode, which should be compared with the second-order result derived from $\epsilon_k^{(\beta)}$, Eqs. (60), (63) and (68), at $k = 0$: $\Delta = (1 + \sqrt{2}q_2)J \simeq 1.676J$, in full agreement with similar spin-wave calculations for AB_2 [19] and spin-1/2-spin-1 [64, 65] chains, and in agreement with numerical estimates using exact diagonalization, $\Delta = 1.759J$, for both AB_2 [5] and spin-1/2-spin-1 [63] chains. On the other hand, the LSWT predicts a gap $\Delta_{flat} = J$ for the flat ferromagnetic mode ($\epsilon_k^{(\xi)}$) in AB_2 chain, whereas our second-order spin-wave theory finds, using Eqs. (60), (64) and (68): $\Delta_{flat} = (1 - 2q_1 + \sqrt{2}q_2)J \simeq 1.066J$, in full agreement with a similar spin-wave procedure [19]. Surprisingly, the estimated value from Exact Diagonalization (ED) [5]: $\Delta_{flat} = 1.0004J$, lies between these two theoretical values. In fact, analytical approaches are still unable to reproduce the observed level crossing found in numerical calculations [5, 19] for the two ferromagnetic modes. This is probably due to the fact that the different symmetries exhibited by the localized excitation (flat mode) and the ferromagnetic dispersive mode are not explicitly manifested in the analytical approaches, so the levels avoid the crossing.

B. Ground state energy

In the thermodynamic limit, the second-order result for the GS energy of the AB_2 chain per unit cell reads:

$$\frac{E_{GS}^J}{N_c} = -4JS^2 + \frac{JS}{2\pi} \int_{-\pi}^{\pi} dk \left(\sqrt{9 - 8\gamma_k^2} - 3 \right) - 2J(q_1^2 + q_2^2 - \frac{3}{\sqrt{2}}q_1q_2). \quad (69)$$

We remark that, at half filling, we shall not consider the constant term $-JN_c$ in Eq. (51), with the purpose of comparison with preceding results. Performing the integration over the first BZ and taking $S = 1/2$, we obtain that the GS energy per site at zero-field is given by $-0.4869J$. This result agrees very well with values obtained using exact diagonalization [45] ($-0.485J$) and DMRG [67] ($-0.4847J$) techniques. For the spin-1/2 - spin-1 chain, the value obtained using DMRG [62] is $-0.72704J$. To compare it with our finding, we need to multiply this value by $2/3$ (ratio between the number of sites of the two chains), yielding $-0.48469J$.

C. Sublattice magnetizations and Lieb GS total spin per unit cell

In order to derive results beyond LSWT, we introduce staggered magnetic fields coupled to spins $S_i^{A,z}$ and $S_i^{B_l,z}$, with $l = 1, 2$, through the Zeeman terms: $-h_A \sum_i S_i^{A,z}$ and $-h_{B_l} \sum_i S_i^{B_l,z}$, which are added to \mathcal{H}_{eff}^J in Eq. (47). Thus, $\langle S^{A,z} \rangle$ and $\langle S^{B_l,z} \rangle$ corresponding to sublattices A and B_l are obtained from $\langle S^{A,z} \rangle = -(1/N_c) \sum_{i=1,2} [\partial E_i(h_A)/\partial h_A]|_{h_A=0}$, and an analogous equation for $\langle S^{B_l,z} \rangle$ using Eqs. (59) and (62):

$$\begin{aligned} (\langle S^{A,z} \rangle, \langle S^{B_l,z} \rangle) &= \mp S \pm \left(\frac{1}{2}, \frac{1}{4} \right) \frac{1}{\pi} \int_{-\pi}^{\pi} dk v_k^2 \\ &\mp \left(\frac{1}{2}, \frac{1}{4} \right) \frac{q_1}{\pi S} \int_{-\pi}^{\pi} dk \frac{\gamma_k^2}{(9 - 8\gamma_k^2)^{3/2}} + \mathcal{O}\left(\frac{1}{S^2}\right). \end{aligned} \quad (70)$$

Carrying out the above integration, we obtain $\langle S^{A,z} \rangle = -0.316343$ and $\langle S^{B_l,z} \rangle = 0.408172$. These results are in good agreement with those obtained using DMRG [11] and ED [5] techniques: $\langle S^{A,z} \rangle = -0.2925$ and $\langle S^{B_l,z} \rangle = 0.3962$, respectively, and with values for $\langle S^{A,z} \rangle$ and $2\langle S^{B_l,z} \rangle$ for the spin-1/2 - spin-1 chain [62-65]. Although at zero temperature, the sublattice magnetizations are strongly reduced by quantum fluctuations, as compared with their classical values, the unit cell magnetization remains $S_L \equiv 1/2$, where S_L is the Lieb GS total spin per unit cell, in full agreement with Lieb's theorem [5, 15] for bipartite lattices:

$$S_L = \frac{1}{2} \|N_A - N_B\|, \quad (71)$$

with $N_A(N_B)$ denoting the total number of spins in sublattice $A(B)$ per unit cell.

V. t - J HAMILTONIAN: DOPING-INDUCED PHASES, GROUND STATE ENERGY AND TOTAL SPIN

In this section, we shall derive the corresponding t - J Hamiltonian suitable to describe the strongly correlated AB_2 Hubbard chain in the doped regime, in which case both charge (Grassmann fields) and spin [$SU(2)$ gauge fields] quantum fluctuations are considered on an equal footing. Indeed, the t - J Hamiltonian can be derived by means of the following Legendre transformation to Eq. (41):

$$\mathcal{H}_{eff}^{t-J} = - \sum_{i,\mu=b,d,e} \frac{\partial \mathcal{L}_{eff}}{\partial (\partial_\tau U_i^{(\mu)})_{\sigma,\sigma}} (\partial_\tau U_i^{(\mu)})_{\sigma,\sigma} - \sum_{i,\nu_i} \frac{\partial \mathcal{L}_{eff}}{\partial (\partial_\tau \nu_i)} \partial_\tau \nu_i + \mathcal{L}_{eff}, \quad (72)$$

where $\frac{\partial \mathcal{L}_{eff}}{\partial (\partial_\tau \nu_i)} = \nu_i^\dagger$ with $\nu_i = \alpha_i, \alpha_i^{\frac{1}{2}}, e_{i\uparrow}$; $\frac{\partial \mathcal{L}_{eff}}{\partial (\partial_\tau U_i^{(b)})_{\sigma,\sigma}} = \theta(-\sigma)(U_i^{(b)\dagger})_{\sigma,\sigma} \alpha_i^{\frac{1}{2}\dagger} \alpha_i^{\frac{1}{2}}$, and $\frac{\partial \mathcal{L}_{eff}}{\partial (\partial_\tau U_i^{(d,e)})_{\sigma,\sigma}} = \theta(\sigma) \frac{1}{2} [(U_i^{(d,e)\dagger})_{\sigma,\sigma} (\alpha_i^\dagger \alpha_i + e_{i\uparrow}^\dagger e_{i\uparrow}) + (U_i^{(e,d)\dagger})_{\sigma,\sigma} (\alpha_i^\dagger e_{i\uparrow} + e_{i\uparrow}^\dagger \alpha_i)]$, from which we can write the effective t - J Hamiltonian as

$$\mathcal{H}_{eff}^{t-J} = \mathcal{H}^t + \mathcal{H}^J, \quad (73)$$

where

$$\begin{aligned} \mathcal{H}^t = & -t \sum_{i\sigma} \{ \theta(-\sigma)(U_i^{(b)\dagger} U_i^{(d)})_{\sigma,-\sigma} \alpha_i^{(1/2)\dagger} \alpha_i \\ & + \theta(\sigma)(U_i^{(d)\dagger} U_{i+1}^{(b)})_{\sigma,-\sigma} \alpha_i^\dagger \alpha_{i+1}^{(1/2)} \\ & + \theta(-\sigma)(U_i^{(b)\dagger} U_i^{(e)})_{\sigma,-\sigma} \alpha_i^{(1/2)\dagger} e_{i\uparrow} \\ & + \theta(\sigma)(U_i^{(e)\dagger} U_{i+1}^{(b)})_{\sigma,-\sigma} e_{i\uparrow}^\dagger \alpha_{i+1}^{(1/2)} + \text{H.c.} \}, \end{aligned} \quad (74)$$

and

$$\begin{aligned} \mathcal{H}^J = & -\frac{J}{4} \sum_{i;i'=i,i+1;\sigma} \theta(\sigma) |(U_i^{(d)\dagger} U_{i'}^{(b)})_{\sigma,\sigma}|^2 \alpha_i^\dagger \alpha_i \\ & -\frac{J}{4} \sum_{i;i'=i,i+1;\sigma} \theta(\sigma) |(U_i^{(e)\dagger} U_{i'}^{(b)})_{\sigma,\sigma}|^2 e_{i\uparrow}^\dagger e_{i\uparrow} \\ & -\frac{J}{4} \sum_{i;i'=i,i-1;\sigma} \theta(-\sigma) |(U_i^{(b)\dagger} U_{i'}^{(d)})_{\sigma,\sigma}|^2 \\ & + |(U_i^{(b)\dagger} U_{i'}^{(e)})_{\sigma,\sigma}|^2 \alpha_i^{\frac{1}{2}\dagger} \alpha_i^{\frac{1}{2}}. \end{aligned} \quad (75)$$

Notice that Eqs. (74) and (75) are identical to Eqs. (42c) and (42d), since Eqs. (42a) and (42b) were eliminated through the Legendre transformation.

Some digression on \mathcal{H}_{eff}^{t-J} is in order. One of the key properties of quasi-1D interacting quantum systems is the phenomenon of spin-charge separation, leading to the formation of spin and charge-density waves, which move independently and with different velocities. It has been demonstrated [24] that for $\delta > 2/3$ the low-energy physics of the doped AB_2 Hubbard chain in the $U = \infty$ coupling limit is described in

terms of the Luttinger-liquid model, with the spin and charge degrees of freedom decoupled. Most importantly, it has been shown that for the AB_2 t - J Hubbard chains [25] charge and spin quantum fluctuations are practically decoupled, as suggested by the emergence of charge-density waves in anti-phase with the modulation of the ferrimagnetic order. One can make use of this feature to formally split each term of the t - J Hamiltonian, Eq. (73)-(75), into a product of two independent terms acting on different Hilbert spaces, i.e., we can enforce spin-charge separation and calculate the charge and spin correlation functions in a decoupled fashion.

Therefore, from the above discussion, we shall consider that the charge correlation functions are well described by an effective spinless tight-binding model [24, 55, 68], since the hole (charge) density waves develop along the x -axis and in anti-phase with the modulation of the ferrimagnetic structure, as numerically observed in Fig. 2(b) of Ref. [25]. So, using Eqs. (33), with $a/2 \rightarrow a$ (effective lattice spacing of the linear chain: distance between A and B sites, see Fig. 2(a) of Ref. [25]), we find

$$\begin{aligned} \langle \alpha_i^{(1/2)\dagger} \alpha_i \rangle &= \frac{1}{N_c} \sum_{kk'} e^{-ik(x_i-1)} e^{ik'x_i} \langle \Psi_0 | \alpha_k^\dagger \alpha_{k'} | \Psi_0 \rangle \\ &= \frac{1}{\pi} \int_{-k_F(\delta)}^{k_F(\delta)} e^{ik} dk = \frac{2}{\pi} \sin[k_F(\delta)], \end{aligned} \quad (76)$$

with $|\Psi_0\rangle$ being the hole-doped ferrimagnetic GS, where $k_F(\delta) = \pi \frac{N_h}{N} \equiv \pi\delta$ is the Fermi wave vector of the spinless tight-binding holes. In the same fashion: $\langle \alpha_i^\dagger \alpha_{i+1}^{(1/2)} \rangle = \frac{2}{\pi} \sin[k_F(\delta)]$ and $\langle \alpha_i^{(1/2)\dagger} e_{i\uparrow} \rangle = \langle e_{i\uparrow}^\dagger \alpha_{i+1}^{(1/2)} \rangle = 0$; while $\langle \alpha_i^\dagger \alpha_i \rangle = \langle \alpha_i^{(1/2)\dagger} \alpha_i^{(1/2)} \rangle = \langle e_{i\uparrow}^\dagger e_{i\uparrow} \rangle = (1 - \frac{1}{2\pi} \int_{-k_F(\delta)}^{k_F(\delta)} dk) = (1 - \delta)$. Here, we remark that the itinerant holes away from half filling are associated with the lower-energy dispersive α_k and $\alpha_k^{(1/2)}$ bands [see Fig. 1(b) in Sec. (II)], thus contributing to the kinetic Hamiltonian in Eq. (74). On the other hand, the local correlations related to the lower-energy bands α_k , $\alpha_k^{(1/2)}$, and $e_{k\uparrow}$, contribute equally to the exchange Hamiltonian in Eq. (75). Thereby, using the above tight-binding results for the charge correlation functions, \mathcal{H}_{eff}^{t-J} in Eqs. (73)-(75) gives rise to the δ -dependent Hamiltonian, $\mathcal{H}_{eff}^{t-J}(\delta) = \mathcal{H}_{eff}^t(\delta) + \mathcal{H}_{eff}^J(\delta)$, written below:

$$\begin{aligned} \mathcal{H}_{eff}^{t-J}(\delta) = & -t \frac{2}{\pi} \sin[k_F(\delta)] \sum_i [(U_i^{(b)\dagger} U_i^{(d)})_{\downarrow\uparrow} \\ & + (U_i^{(d)\dagger} U_{i+1}^{(b)})_{\uparrow\downarrow} + \text{H.c.}] \\ & - \frac{J(1-\delta)}{4} \sum_{\langle i\alpha,j\beta \rangle \sigma} \theta(p_{i\alpha}\sigma) |(U_{i\alpha}^\dagger U_{j\beta})_{\sigma,\sigma}|^2, \end{aligned} \quad (77)$$

where the sum over σ was evaluated in Eq. (74) and the square of the $SU(2)$ gauge field products in the exchange contribution have been summed up in Eq. (75), so that this contribution is just $(1 - \delta)$ times \mathcal{H}_{eff}^J at half filling, Eq. (45), or alternatively, in terms of spin fields, Eq. (47), or spin-waves, Eqs. (66)-(68). On the other hand, the $SU(2)$ gauge fields ma-

trix elements: $(U_i^{(b)\dagger}U_i^{(d)})_{\downarrow\uparrow}$ and $(U_i^{(d)\dagger}U_{i+1}^{(b)})_{\uparrow\downarrow}$, that appear in the kinetic contribution of Eq. (77), can be written in terms of the spin fields [55, 56] as

$$(U_i^{(b)\dagger}U_i^{(d)})_{\downarrow\uparrow} + \text{H.c.} = \sum_l \frac{1}{\sqrt{2}} \left(\sqrt{1 - 2S_i^{B_l,z} - 2S_i^{A,z} + 4S_i^{A,z}S_i^{B_l,z}} + \sqrt{1 + 2S_i^{A,z} + 2S_i^{B_l,z} + 4S_i^{A,z}S_i^{B_l,z}} \right), \quad (78)$$

and $(U_i^{(d)\dagger}U_{i+1}^{(b)})_{\uparrow\downarrow}$ is obtained from Eq. (78) through the replacement $S_i^{A,z} \rightarrow S_{i+1}^{A,z}$, in which case we took advantage of the $U(1)$ gauge freedom and Eq. (46). Notice that these square-root matrix elements depend on z -spin components only.

At this stage, it will prove useful, in the calculation of the GS total spin in the doped regime, to consider $\mathcal{H}_{eff}^{t-J}(\delta, h)$ which describes the system in the presence of a homogeneous magnetic field $\mathbf{h} = h\hat{\mathbf{z}} = (-h_A + h_{B_1} + h_{B_2})\hat{\mathbf{z}}$, where the staggered fields point along the local corresponding magnetizations in the ferrimagnetic phase have the same magnitude h . The magnetic field couple with the spin fields through the Zeeman term (see Sec. IV C) and with the charge degrees of freedom through the magnetic orbital coupling in the Landau gauge: $\mathbf{A} = h x \hat{\mathbf{y}}$. Since our aim is to study doping effect on the magnetization, we shall assume vanishingly small magnetic field in the context of linear response theory and perturbative expansion in the strong-coupling regime. Additionally, the magnetic orbital coupling can be considered through the so-called Peierls substitution [27, 69]: $t \rightarrow t e^{i \int_{i\alpha}^{j\beta} \mathbf{A} \cdot d\mathbf{l}}$, where $i\alpha$ and $j\beta$ are first-neighbor sites, and the flux quantum $\phi_0 = hc/e \equiv 1$. If one consider that the carrier is at the site iA , we have four hopping possibilities: $iA \rightarrow iB_{1,2}$ and $iA \rightarrow (i+1)B_{1,2}$, so the total phase ϕ acquired by the carrier in this prescription satisfies Stokes' theorem: $\phi = \oint_{\text{unit cell}} \mathbf{A} \cdot d\mathbf{l} = \iint_S \mathbf{h} \cdot d\mathbf{S} = ha^2$ ($a \equiv 1$). We also remark that, in order to obtain real values for the zero-field staggered magnetizations, we have considered, for convenience, an imaginary gauge transformation [56, 70]: $\mathbf{A} \rightarrow i\mathbf{A}$. Therefore, by placing Eq. (78) and the similar matrix element into the kinetic term in Eq. (77), making the above Peierls substitution, and using the Holstein-Primakoff and Bogoliubov transformations introduced in Eqs. (48)-(50) and Eqs. (56)-(57), respectively, up to order $\mathcal{O}(S^{-1})$, we arrive at the following diagonalized kinetic Hamiltonian $\mathcal{H}_{eff}^t(\delta, h)$:

$$\mathcal{H}_{eff}^t(\delta, h) = -\frac{4\sqrt{2}}{\pi} t e^{-(h_A + h_{B_1} + h_{B_2})} \sin[k_F(\delta)] \sum_k [4S - 3v_k^2 - (u_k^2 + 2v_k^2)\alpha_k^\dagger\alpha_k - (2u_k^2 + v_k^2)\beta_k^\dagger\beta_k - \xi_k^\dagger\xi_k], \quad (79)$$

where the doped-induced contributions for the spin dispersion relations are evidenced in the last three terms. On the other hand, by adding the Zeeman terms (see Sec. IV C) to the exchange contribution $\mathcal{H}_{eff}^J(\delta)$, given in Eq. (77), we obtain $\mathcal{H}_{eff}^J(\delta, h)$. Lastly, by adding the kinetic and the exchange contributions, we arrive at the effective t - J Hamiltonian in the presence of a magnetic field:

$$\begin{aligned} \mathcal{H}_{eff}^{t-J}(\delta, h) = & -\frac{4\sqrt{2}}{\pi} t e^{-(h_A + h_{B_1} + h_{B_2})} \sin[k_F(\delta)] \sum_k (4S - 3v_k^2) + J(1 - \delta)(E_{GS}^J - JN_c) \\ & + \sum_k [\epsilon_k^{(\alpha)}(\delta)\alpha_k^\dagger\alpha_k + \epsilon_k^{(\beta)}(\delta)\beta_k^\dagger\beta_k + \epsilon_k^{(\xi)}(\delta)\xi_k^\dagger\xi_k] - h_A \sum_i S_i^{A,z} - h_{B_1} \sum_i S_i^{B_{1,z}} - h_{B_2} \sum_i S_i^{B_{2,z}}, \end{aligned} \quad (80)$$

where E_{GS}^J is given by Eq. (67) and (69), and the corresponding spin-wave modes [see Eqs. (79), (60), (63)-(65), and (68)] of the doped AB_2 t - J chain read:

$$\epsilon_k^{(\alpha)}(\delta) = \frac{4\sqrt{2}}{\pi} t \sin(\pi\delta) [u_k^2 + 2v_k^2] + (1 - \delta)(\epsilon_k^{0(\alpha)} + \delta\epsilon_k^{(\alpha)}), \quad (81)$$

$\epsilon_k^{(\beta)}(\delta)$ is obtained from $\epsilon_k^{(\alpha)}(\delta)$ through the exchange $u_k \leftrightarrow v_k$ and the replacement $\alpha \rightarrow \beta$, while

$$\epsilon_k^{(\xi)}(\delta) = \frac{4\sqrt{2}}{\pi} t \sin(\pi\delta) + (1 - \delta)(\epsilon_k^{0(\xi)} + \delta\epsilon_k^{(\xi)}). \quad (82)$$

We find it instructive to comment on the analytical structure of the above equations. Firstly, we mention the presence of the Bogoliubov parameters [see Eqs. (57)] in a symmetric form in the kinetic terms of Eq. (81) and its analogous for $\epsilon_k^{(\beta)}(\delta)$; besides, although the flat mode is strongly affected by the presence of holes, it remains dispersionless. In addition, using Eqs. (80) and (65), the total GS energy (no spin-wave excitations) per unit cell in the thermodynamic limit is readily obtained:

$$\begin{aligned} E_{GS}^{t-J}(\delta, h)/N_c = & -\frac{4\sqrt{2}}{\pi} t e^{-(h_A + h_{B_1} + h_{B_2})} \sin(\pi\delta) (4S - 3q_1) \\ & + (1 - \delta)(E_{GS}^J/N_c - J) - \langle S^{A,z} \rangle h_A - \sum_{l=1,2} \langle S^{B_l,z} \rangle h_{B_l}, \end{aligned} \quad (83)$$

where $\langle S^{A,z} \rangle$ and $\langle S^{B,z} \rangle$ are the calculated sublattice magnetizations, at half filling and zero-field, given by Eqs. (70).

In subsections **VA**, **VB**, and **VC**, we will show that the underlying competing physical mechanisms: the magnetic orbital response and the Zeeman contribution embedded in Eqs. (80)-(83) will dramatically affect the behavior of the system under hole doping and, in particular, will lead to spiral IC spin structures, the breakdown of the spiral ferrimagnetic GS at a critical value of the hole doping, a region of phase separation, and RVB states at $\delta \approx 1/3$.

A. Doped regime: Spin-wave modes

Before we go one step further to discuss relevant macroscopic quantities, i.e., the GS energy and total spin in the doped regime, we shall first undertake a detailed study, at a microscopic level, of the hole-doping effect on the calculated spin-wave branches given by Eqs. (81)-(82).

Fig. 2 depicts the second-order spin-wave dispersion relations at $J/t = 0.3$ and for the indicated values of δ . Without loss of generality, we set $t = 1$ in our numerical computations. At half filling, the antiferromagnetic mode $\epsilon_k^{(\beta)}$, together with the two ferromagnetic modes: the dispersive $\epsilon_k^{(\alpha)}$ and the flat one $\epsilon_k^{(\xi)}$, are shown in Fig. 2(a), which are defined in Eq. (68), and can be plotted using Eqs. (60) and (63)-(65).

As the hole doping increases slightly, the abrupt decrease of the peaks at $k = 0$ and $k = \pi$ of the numerical DMRG structure factor (see Fig. 3 of Ref. [25]), associated with the ferrimagnetic order, manifests itself here through the opening of a gap in the ferromagnetic Goldstone mode $\epsilon_k^{(\alpha)}$, as seen in Fig. 2(b), thus indicating that the system loses its long-range order. Note that the antiferromagnetic mode $\epsilon_k^{(\beta)}$ is also similarly shifted. On the other hand, although the dispersion relation is modified for small values of the wave vector k , the minimum value of $\epsilon_k^{(\alpha)}$ still remains at $k = 0$ up to the *onset* of the formation of spiral IC spin structures at $\delta_c(\text{IC}) = 0.043$ (a value that should be compared with the numerical DMRG estimate of $\delta \approx 0.055 \pm 0.012$), characterized by the flattening of the dispersive spin-wave branches around zero. Upon further increase of δ , two minima form (around $k = 0$) and move away from each other as one enhances the hole doping. This behavior is the signature of the occurrence of spiral IC spin structures (see Fig. 3 of Ref. [25]).

Fig. 2(c) shows the onset of phase separation (PS) at $\delta(\text{PS}) = 0.165$ for $J = 0.3$, which is characterized by the overlap of the two ferromagnetic modes at $k = 0$. The signature of this regime is the spatial coexistence of two phases: spiral IC spin structures at $\delta(\text{PS}) = 0.165$ and RVB states at $\delta \approx 1/3$, in very good agreement with the numerical estimate of $\delta_{\text{IC-PS}} \approx 0.16$ [25]. At $\delta \approx 1/3$, the flat mode has the lowest energy, as illustrated in Fig. 2(d). This behavior indicates that the RVB state is the stable phase at $\delta \approx 1/3$ and $J = 0.3$ [25], and also in agreement with the numerical DMRG studies [11, 24] and analytical prediction at $U = \infty$ [55].

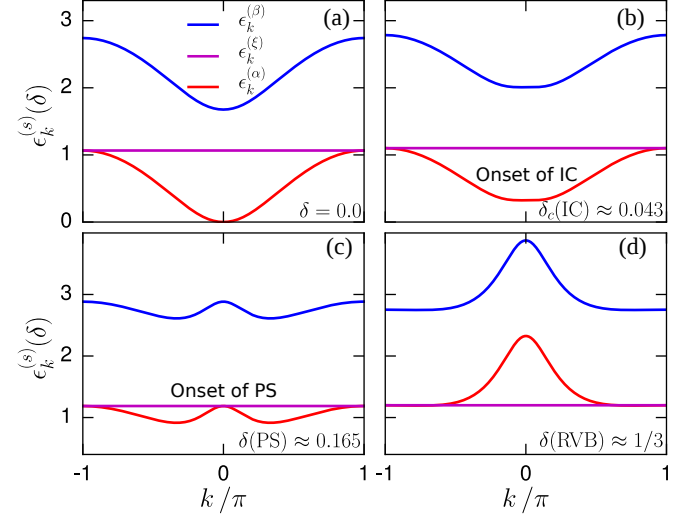


Figure 2. (Color online) Evolution of the zero-field second-order spin-wave dispersion relations of the AB_2 t - J chain as a function of hole doping (δ): dispersive ferromagnetic $\epsilon_k^{(\alpha)}$ and antiferromagnetic $\epsilon_k^{(\beta)}$ modes and the flat ferromagnetic one $\epsilon_k^{(\xi)}$, at (a) half filling; (b) the onset of the spiral IC spin structures at $\delta_c(\text{IC}) = 0.043$, in which case the flattening of the gap of $\epsilon_k^{(\alpha)}$ around $k = 0$ is observed; (c) the onset of PS at $\delta(\text{PS}) = 0.165$, characterized by the overlap of the two ferromagnetic modes at $k = 0$ and by the spatial coexistence of two phases: spiral IC spin structures, with modulation fixed at $\delta(\text{PS})$, and RVB states at $\delta \approx 1/3$. (d) At $\delta = 1/3$ the flat mode presents the lowest energy, thus indicating that the short-range RVB state is the stable phase.

In order to better understand the rich variety of doping-induced phases in the system, in Fig. 3 we plot the evolution of the wave vector k_{\min} corresponding to the local minimum of $\epsilon_k^{(\alpha)}(\delta)$, upon increasing the hole doping δ from 0 to $1/3$. The wave vector k_{\min} remains zero until it hits the onset doping value $\delta_c(\text{IC}) = 0.043$, beyond which a square-root growth behavior takes place [71]: $[\delta - \delta_c(\text{IC})]^{1/2}$ (blue line), for δ close to $\delta_c(\text{IC})$. The square-root growth behavior is the signature of the occurrence of a second-order quantum phase transition from the doped ferrimagnetic phase to the IC spiral ferrimagnetic state with a non-zero value of the total GS spin, S_{GS} . This result is supported by the behavior of $\Delta_k \equiv k_{\max} - \pi$ at which the local maximum of the numeric DMRG structure factor $S(k)$ near $k = \pi$ is observed, as shown in the inset of Fig. 3 (taken from the inset of Fig. 3(b) of Ref. [25]). For further increase of hole doping our result deviates from the square-root growth behavior and some very interesting features are to be noticed. The value of $\delta_c = 0.08$ indicates the breakdown of the total S_{GS} in the IC phase, as will be confirmed by the explicit calculation of S_{GS} , a macroscopic quantity, in Section **VC**. Thus, for $0.08 < \delta < 0.165$ the system displays an IC phase with zero S_{GS} , in agreement with the DMRG data (see Fig. 1(c) of Ref. [25]). At $\delta(\text{PS}) = 0.165$

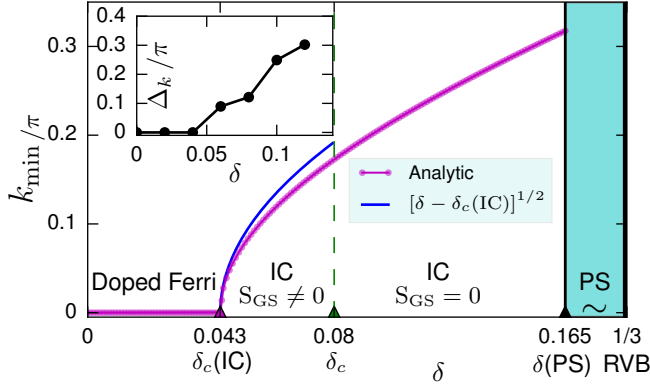


Figure 3. (Color online) Evolution of k_{\min} (value of k at the local minimum of $\epsilon_k^{(\alpha)}(\delta)$ near $k = 0$) as a function of δ : doped ferrimagnetism for $0 < \delta < \delta_c(\text{IC}) \approx 0.043$; spiral IC spin structures with non-zero (zero) S_{GS} for $\delta_c(\text{IC}) < \delta < \delta_c \approx 0.08$ ($\delta_c < \delta < \delta(\text{PS}) \approx 0.165$), with a second-order quantum phase transition at $\delta_c(\text{IC})$ characterized by a square-root behavior $[\delta - \delta_c(\text{IC})]^{1/2}$ (blue line), and a first-order transition at $\delta(\text{PS})$ involving the IC spin structure, with modulation fixed at $\delta(\text{PS})$, and short-range RVB states at hole concentration $1/3$. The inset shows DMRG data from Ref. [25] for $\Delta_k \equiv k_{\max} - \pi$ as a function of δ , where k_{\max} is the value of k at the local maximum of the structure factor $S(k)$ near $k = \pi$, in qualitative agreement with the second-order transition at $\delta_c(\text{IC})$.

the system exhibits a first-order transition accompanied by the spatial phase separation regime: the IC phase with zero S_{GS} and modulation fixed by $\delta(\text{PS})$ in coexistence with the short-range RVB states at $\delta \approx 1/3$, also consistent with the DMRG data plotted in Fig. 4 of Ref. [25].

Lastly, we emphasize that, despite the occurrence of several doping-induced phases in the DMRG studies [25]: Lieb ferrimagnetism, spiral IC spin structures, RVB states with finite spin gap, phase separation, and Luttinger-liquid behavior, it is surprising and very interesting that the second-order spin-wave modes remain stable up to $\delta \approx 1/3$, with predictions in very good agreement with the DMRG studies [25]. In this context, it is worth mentioning the long time studied case of rare earth metals [72], where an external magnetic field can induce non-trivial phase transitions involving spiral spin structures, well described by spin-wave theory.

B. Doped regime: Ground state energy

Performing the integration over the first BZ in Eqs. (65) and (69) and setting $S = 1/2$ in Eq. (83), we find that the AB_2 t - J ground state energy per unit cell as a function of hole doping in zero-field reads:

$$E_{GS}^{t-J}(\delta)/JN_c = -1.9543 \frac{t}{J} \sin(\pi\delta) - 2.4608(1 - \delta). \quad (84)$$

We shall now examine the case of small hole doping away from half filling, i.e., with hole concentration ranging from $\delta = 0$ up to $\delta = 0.2$ for two values of J : 0.1 and 0.3. In Fig. 4, we show the evolution of the GS energy per unit cell

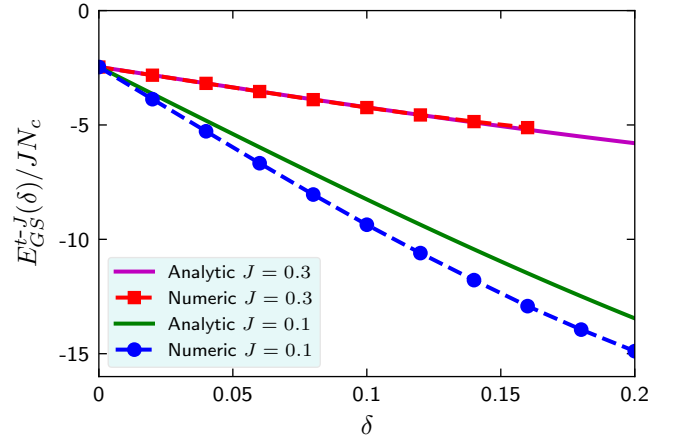


Figure 4. (Color online) Analytical prediction for the GS energy per unit cell of the AB_2 t - J chain as a function of doping, and comparison with numerical data from DMRG technique for $J/t = 0.1$ and $J/t = 0.3$ [25]. At half filling ($\delta = 0$), both results meet at the expected prediction [25]: ≈ -2.4678 . Note that we have added the term $-JN_c$ with the intention of comparison with numerical calculation.

of the AB_2 t - J model as a function of hole doping for both mentioned values of J , and the comparison was made with the numerical DMRG data [25]. From the two results at $J = 0.3$, the only quantitative difference induced by the increase of the hole concentration is a crossing feature around $\delta \approx 0.1$, where our analytical result slightly change its behavior by lowering the energy with respect to the numerical data [25]. In fact, because our model assumes a ferrimagnetic state as the starting point, this change of behavior suggests that we have entered in a region of strong magnetic instabilities, and possibly indicating a smooth transition to an incommensurate phase with zero GS total spin beyond $\delta \approx 0.1$, as confirmed by the numerical data in Ref. [25] and illustrated in Fig. 3. On the other hand, at $J = 0.1$, although our results reproduce the numerical data with an acceptable agreement, we observe a discrepancy that increases with δ . The cause of such discrepancy will be discussed in the next subsection.

With the purpose of determining the interplay between the contribution of magnetic exchange and the itinerant kinetic energy to the zero-field GS energy Eq. (83), we take $J = 0.3$ and show its evolution with doping in Fig. 5. We can see in the insets, Fig. 5(a) and Fig. 5(b), the competitive behavior of the two energetic contributions, i.e., the contribution of the exchange energy increases linearly with δ , while a practically linear decrease of the hopping term is observed as one enhances the hole doping. This competition indicates that a phase transition to a paramagnetic phase should occur at some critical concentration value.

C. Doped regime: Ground state total spin

The existence of a transition from an IC spiral ferrimagnetic phase to an IC paramagnetic one is a most interest-

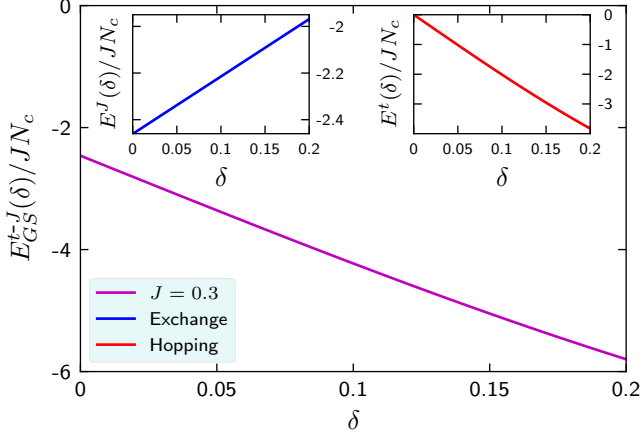


Figure 5. (Color online) Ground-state energy per unit cell for the AB_2 t - J chain as a function of δ for $J = 0.3$. In the insets, we illustrate the two energetic contribution due to (a) exchange and (b) hopping terms.

ing feature observed numerically in doped AB_2 t - J Hubbard chains [25]. In order to firmly corroborate the mentioned transition, we have calculated the GS total spin per unit cell as a function of hole doping, $S_{GS}(\delta) = \sum_{\alpha} \langle S^{\alpha,z} \rangle(\delta)$, with $\alpha = A, B_1, B_2$, by means of the zero-field derivative of Eq. (83):

$$\langle S^{\alpha,z} \rangle(\delta) = -(1/N_c)[\partial E_{GS}^{t-J}(\delta, h)/\partial h_{\alpha}]|_{h_{\alpha}=0}. \quad (85)$$

We thus find

$$\langle S^{\alpha,z} \rangle(\delta) = \langle S^{\alpha,z} \rangle \pm \frac{4\sqrt{2}}{\pi} t \sin(\pi\delta)(4S - 3q_1), \quad (86)$$

where $+$ ($-$) corresponds to sublattice $\alpha = A$ ($\alpha = B_{1,2}$), and $\langle S^{A,z} \rangle$ and $\langle S^{B_{1,2},z} \rangle$ are given by Eqs. (70). Therefore, by performing the integration over the first BZ of the three contributions in Eq. (86), we finally obtain:

$$\frac{S_{GS}(\delta)}{S_L} = 1 - 3.9086 \sin(\pi\delta), \quad (87)$$

where $S_L = \sum_{\alpha} \langle S^{\alpha,z} \rangle = 1/2$ is Lieb's reference value for the GS total spin per unit cell at half filling and zero-field (see Section IV C).

In Fig. 6 we plot the evolution of S_{GS} , normalized by S_L , as a function of δ , and compare it with the numerical data from DMRG and Lanczos techniques [25], for $J = 0.3$ (red squares) and $J = 0.1$ (blue circles). In the latter (former) case, the system undergoes a transition from the modulated itinerant ferrimagnetic phase to an incommensurate phase with zero (nonzero) S_{GS} . Notice that, in both cases, the transition is characterized by a decrease of S_{GS} from S_L to 0 or to a residual value, regardless of the value that S_{GS} takes after the transition. Indeed, at $J = 0.1$ and $\delta > 0.1$, the formation of magnetic polarons (onset of the Nagaoka phenomena that sets in as $U \rightarrow \infty$) with charge-density waves in phase with the modulation of the ferrimagnetic structure, as indicated by

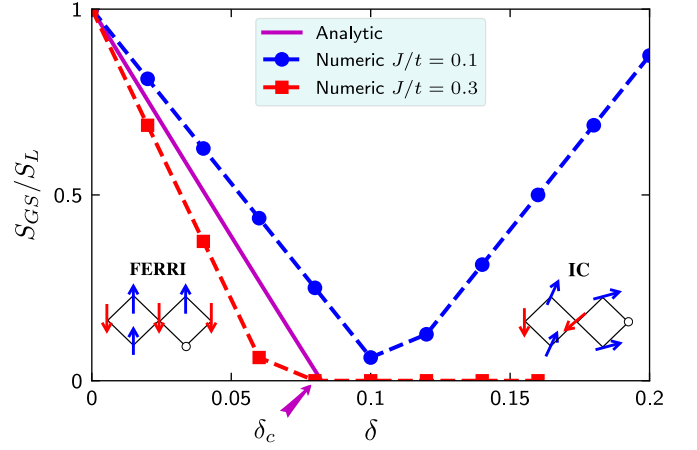


Figure 6. (Color online) Ground-state total spin S_{GS} per unit cell (solid magenta line), normalized by its value in the undoped regime: $S_L = \frac{1}{2}$, as a function of hole doping δ for the indicated values of J . In the figure, $\delta_c \approx 0.08$ indicates the critical value of doping at which the magnetic order is suppressed and a second-order phase transition takes place.

the DMRG data [25], leads to an incommensurate phase with nonzero S_{GS} .

Most importantly, we can observe in Fig. 6 that the value of S_{GS} decreases practically linearly with δ until the magnetic order is completely suppressed at $\delta_c \approx 0.08$. This behavior is supported by numerical results [25], particularly in the regime where the Nagaoka phenomenon is not manifested, that is, at $J = 0.3$, as indicated in Fig. 3. In this regime, spin and charge quantum fluctuations destabilize the ferrimagnetic structure and trigger a transition to an incommensurate paramagnetic phase at δ_c , with $S_{GS} \sim (\delta - \delta_c) \rightarrow 0$.

VI. CONCLUSIONS

In summary, we have presented a detailed analytical study of the large- U Hubbard model on the quasi-one-dimensional AB_2 chain. We used a functional integral approach combined with a perturbative expansion in the strong-coupling regime that allowed us to properly analyze the referred system at and away from half filling.

At half filling, our model was mapped onto the quantum Heisenberg model, and analyzed through a spin-wave perturbative series expansion in powers of $1/S$. We have demonstrated that the GS energy, spin-wave modes, and sublattice magnetizations are in very good agreement with previous results. In the challenging hole doping regime away from half filling, the corresponding t - J ($= 4t^2/U$) Hamiltonian was derived. Further, under the assumption that charge and spin quantum correlations are decoupled, the evolution of the second-order spin-wave modes in the doped regime has unveiled the occurrence of spatially modulated spin structures and the emergence of phase separation (first-order transition) in the presence of resonating-valence-bond states. The doping-dependent GS energy and total spin per unit cell are

also calculated, in which case the collapse of the spiral magnetic order at a critical hole concentration was observed. Remarkably, our above-mentioned analytical results in the doped regime are in very good agreement with density matrix renormalization group studies, where our assumption of spin-charge decoupling is numerically supported by the formation of charge-density waves in anti-phase with the modulation of the ferrimagnetic structure.

Finally, we stress that our reported results evidenced that the present approach, also used in a study on the compatibility between numerical and analytical outcomes of the large-U Hubbard model on the honeycomb lattice, was proved suitable

for the AB_2 chain (a quasi-1D system), where the impact of charge and spin quantum fluctuations are expected to manifest in a stronger way. We thus conclude that our approach offers a quite powerful analytical description of hole-doping induced phases away from half filling in low-dimensional strongly-correlated electron systems.

ACKNOWLEDGMENTS

We appreciate interesting discussions with R. R. Montenegro-Filho. This work was supported by CNPq, CAPES and FACEPE/PRONEX (Brazilian agencies).

-
- [1] S. Sachdev, *Quantum Phase Transitions*, 2nd ed. (Cambridge University Press, 2011).
 - [2] M. A. Continentino, *Quantum scaling in many-body systems*, 2nd ed. (Cambridge University Press, 2017).
 - [3] M. D. Coutinho-Filho, R. R. Montenegro-Filho, E. P. Raposo, C. Vitoriano, and M. H. Oliveira, *J. Braz. Chem. Soc.* **19**, 232 (2008).
 - [4] N. B. Ivanov, *Condensed Matter Phys* **12** (2009).
 - [5] R. R. Montenegro-Filho and M. D. Coutinho-Filho, *Physica A* **357**, 173 (2005).
 - [6] J. Silvestre and R. Hoffmann, *Inorg. Chem.* **24**, 4108 (1985).
 - [7] A. M. S. Macêdo, M. C. dos Santos, M. D. Coutinho-Filho, and C. A. Macêdo, *Phys. Rev. Lett.* **74**, 1851 (1995).
 - [8] G.-S. Tian and T.-H. Lin, *Phys. Rev. B* **53**, 8196 (1996).
 - [9] F. C. Alcaraz and A. L. Malvezzi, *J. Phys. A* **30**, 767 (1997).
 - [10] E. P. Raposo and M. D. Coutinho-Filho, *Phys. Rev. Lett.* **78**, 4853 (1997); *Phys. Rev. B* **59**, 14384 (1999).
 - [11] G. Sierra, M. A. Martín-Delgado, S. R. White, D. J. Scalapino, and J. Dukelsky, *Phys. Rev. B* **59**, 7973 (1999).
 - [12] M. A. Martín-Delgado, J. Rodríguez-Laguna, and G. Sierra, *Phys. Rev. B* **72**, 104435 (2005).
 - [13] E. Lieb and D. Mattis, *J. Math. Phys.* **3**, 749 (1962).
 - [14] E. H. Lieb and F. Y. Wu, *Phys. Rev. Lett.* **20**, 1445 (1968).
 - [15] E. H. Lieb, *Phys. Rev. Lett.* **62**, 1201 (1989).
 - [16] E. H. Lieb, in *The Hubbard Model: Its Physics and Mathematical Physics*, Nato ASI, Series B: Physics, edited by D. Baeriswyl, D. K. Campbell, J. M. P. Carmelo, F. Guinea and E. Louis, Vol. 343 (Plenum, New York, 1995).
 - [17] H. Tasaki, *J. Phys. Condens. Matter* **10**, 4353 (1998); *Prog. Theor. Phys.* **99**, 489 (1998).
 - [18] G.-S. Tian, *J. Stat. Phys.* **116**, 629 (2004).
 - [19] S. Yamamoto and J. Ohara, *Phys. Rev. B* **76**, 014409 (2007).
 - [20] R. R. Montenegro-Filho and M. D. Coutinho-Filho, *Phys. Rev. B* **78**, 014418 (2008).
 - [21] K. Hida and K. Takano, *Phys. Rev. B* **78**, 064407 (2008).
 - [22] T. Shimokawa and H. Nakano, *Journal of the Physical Society of Japan* **81**, 084710 (2012).
 - [23] S. C. Furuya and T. Giamarchi, *Phys. Rev. B* **89**, 205131 (2014).
 - [24] R. R. Montenegro-Filho and M. D. Coutinho-Filho, *Phys. Rev. B* **74**, 125117 (2006).
 - [25] R. R. Montenegro-Filho and M. D. Coutinho-Filho, *Phys. Rev. B* **90**, 115123 (2014).
 - [26] T. Giamarchi, *Quantum Physics in One Dimension* (Clarendon; Oxford University Press, 2004).
 - [27] F. H. L. Essler, H. Frahm, F. Göhmann, A. Klümper, and V. E. Korepin, *The one-dimensional Hubbard model* (Cambridge University Press, 2005).
 - [28] J. M. P. Carmelo and P. D. Sacramento, *Phys. Rep.* **749** (2018).
 - [29] F. D. M. Haldane, *Phys. Rev. Lett.* **67**, 937 (1991); Y.-S. Wu, *Phys. Rev. Lett.* **73**, 922 (1994).
 - [30] C. Vitoriano, R. R. Montenegro-Filho, and M. D. Coutinho-Filho, *Phys. Rev. B* **98**, 085130 (2018).
 - [31] A. A. Lopes and R. G. Dias, *Phys. Rev. B* **84**, 085124 (2011); A. A. Lopes, B. A. Z. António, and R. G. Dias, *Phys. Rev. B* **89**, 235418 (2014).
 - [32] M. Drillon, M. Belaiche, P. Legoll, J. Aride, A. Boukhari, and A. Moqine, *J. Magn. Magn. Mater* **128**, 83 (1993).
 - [33] A. A. Belik, A. Matsuo, M. Azuma, K. Kindo, and M. Takano, *J. Solid State Chem.* **178**, 709 (2005).
 - [34] M. Matsuda, K. Kakurai, A. A. Belik, M. Azuma, M. Takano, and M. Fujita, *Phys. Rev. B* **71**, 144411 (2005).
 - [35] W. Guo, Z. He, and S. Zhang, *J. Alloys Compd.* **717**, 14 (2017).
 - [36] M. Verdaguier, A. Gleizes, J. P. Renard, and J. Seiden, *Phys. Rev. B* **29**, 5144 (1984).
 - [37] A. S. F. Tenório, R. R. Montenegro-Filho, and M. D. Coutinho-Filho, *J. Phys. Condens. Matter* **23**, 506003 (2011).
 - [38] J. Strečka and T. Verkholyak, *J. Low. Temp. Phys.* **1** (2016); See also: X. Yan, Z.-G. Zhu, and G. Su, *AIP Advances* **5**, 077183 (2015).
 - [39] H. Kikuchi, Y. Fujii, M. Chiba, S. Mitsudo, T. Idehara, T. Tonegawa, K. Okamoto, T. Sakai, T. Kuwai, and H. Ohta, *Phys. Rev. Lett.* **94**, 227201 (2005).
 - [40] M. Oshikawa, M. Yamanaka, and I. Affleck, *Phys. Rev. Lett.* **78**, 1984 (1997).
 - [41] M. Hase, M. Kohno, H. Kitazawa, N. Tsujii, O. Suzuki, K. Ozawa, G. Kido, M. Imai, and X. Hu, *Phys. Rev. B* **73**, 104419 (2006).
 - [42] K. C. Rule, A. U. B. Wolter, S. Süllow, D. A. Tennant, A. Brühl, S. Köhler, B. Wolf, M. Lang, and J. Schreuer, *Phys. Rev. Lett.* **100**, 117202 (2008).
 - [43] F. Aimo, S. Krämer, M. Klanjšek, M. Horvatić, C. Berthier, and H. Kikuchi, *Phys. Rev. Lett.* **102**, 127205 (2009).
 - [44] H. Jeschke, I. Opahle, H. Kandpal, R. Valentí, H. Das, T. Saha-Dasgupta, O. Janson, H. Rosner, A. Brühl, B. Wolf, M. Lang, J. Richter, S. Hu, X. Wang, R. Peters, T. Pruschke, and A. Honecker, *Phys. Rev. Lett.* **106**, 217201 (2011).
 - [45] K. Takano, K. Kubo, and H. Sakamoto, *J. Phys. Condens. Matter* **8**, 6405 (1996).
 - [46] K. Okamoto, T. Tonegawa, Y. Takahashi, and M. Kaburagi, *J. Phys. Condens. Matter* **11**, 10485 (1999).

- [47] K. Okamoto, T. Tonegawa, and M. Kaburagi, *J. Phys. Condens. Matter* **15**, 5979 (2003).
- [48] A. S. F. Tenório, R. R. Montenegro-Filho, and M. D. Coutinho-Filho, *Phys. Rev. B* **80**, 054409 (2009).
- [49] K. Morita, M. Fujihala, H. Koorikawa, T. Sugimoto, S. Sota, S. Mitsuda, and T. Tohyama, *Phys. Rev. B* **95**, 184412 (2017).
- [50] M. Fujihala, H. Koorikawa, S. Mitsuda, K. Morita, T. Tohyama, K. Tomiyasu, A. Koda, H. Okabe, S. Itoh, T. Yokoo, S. Ibuka, M. Tadokoro, M. Itoh, H. Sagayama, R. Kumai, and Y. Murakami, *Sci. Rep.* **7**, 16785 (2017).
- [51] E. Dagotto, *Science* **309**, 257 (2005).
- [52] T.-R. T. Han, F. Zhou, C. D. Malliakas, P. M. Duxbury, S. D. Mahanti, M. G. Kanatzidis, and C.-Y. Ruan, *Sci. Adv.* **1** (2015), 10.1126/sciadv.1400173.
- [53] E. Dagotto, *Rep. Prog. Phys.* **62**, 1525 (1999).
- [54] Z. Y. Weng, D. N. Sheng, C. S. Ting, and Z. B. Su, *Phys. Rev. Lett.* **67**, 3318 (1991); *Phys. Rev. B* **45**, 7850 (1992).
- [55] M. H. Oliveira, E. P. Raposo, and M. D. Coutinho-Filho, *Phys. Rev. B* **80**, 205119 (2009).
- [56] F. G. Ribeiro and M. D. Coutinho-Filho, *Phys. Rev. B* **92**, 045105 (2015).
- [57] Z.-C. Gu, H.-C. Jiang, D. N. Sheng, H. Yao, L. Balents, and X.-G. Wen, *Phys. Rev. B* **88**, 155112 (2013).
- [58] E. Fradkin, *Field theories of condensed matter physics*, 2nd ed. (Cambridge University Press, 2013).
- [59] J. W. Negele and H. Orland, *Quantum many-particle systems*, Frontiers in physics (Addison-Wesley Pub. Co., 1988).
- [60] W. K. Tung, *Group theory in physics* (World Scientific, New York, 1985).
- [61] C. Vitoriano, F. B. D. Brito, E. P. Raposo, and M. D. Coutinho-Filho, *Mol. Cryst. Liq. Cryst.* **374**, 185 (2002).
- [62] S. K. Pati, S. Ramasesha, and D. Sen, *Phys. Rev. B* **55**, 8894 (1997).
- [63] S. Yamamoto, S. Brehmer, and H.-J. Mikeska, *Phys. Rev. B* **57**, 13610 (1998).
- [64] N. B. Ivanov, *Phys. Rev. B* **62**, 3271 (2000).
- [65] S. Yamamoto, *Phys. Rev. B* **69**, 064426 (2004).
- [66] W. M. da Silva and R. R. Montenegro-Filho, *Phys. Rev. B* **96**, 214419 (2017).
- [67] H. Niggemann, G. Uimin, and J. Zittartz, *J. Phys. Condens. Matter* **9**, 9031 (1997).
- [68] C. Vitoriano and M. D. Coutinho-Filho, *Phys. Rev. B* **82**, 125126 (2010).
- [69] J. Vidal, B. Douçot, R. Mosseri, and P. Butaud, *Phys. Rev. Lett.* **85**, 3906 (2000); Z. Gulácsi, A. Kampf, and D. Vollhardt, *Phys. Rev. Lett.* **99**, 026404 (2007).
- [70] N. Hatano and D. R. Nelson, *Phys. Rev. Lett.* **77**, 570 (1996).
- [71] S. Chakrabarty, V. Dobrosavljević, A. Seidel, and Z. Nussinov, *Phys. Rev. E* **86**, 041132 (2012).
- [72] B. R. Cooper and R. J. Elliott, *Phys. Rev.* **131**, 1043 (1963); See also: A. R. Mackintosh and H. B. Møller, *Spin Waves*, in *Magnetic Properties of Rare Earth Metals*, edited by R. J. Elliott (Plenum Press, 1972), Chapter 1, p. 187.